

## Depositional environments and source rock potential of some Upper Palaeozoic (Devonian) coals on Bjørnøya, Western Barents shelf

Julian Janocha<sup>a,b,\*</sup>, Fredrik Wesenlund<sup>c</sup>, Olaf Thießen<sup>d</sup>, Sten-Andreas Grundvåg<sup>a,b</sup>, Jean-Baptiste Koehl<sup>e</sup>, Erik P. Johannessen<sup>f</sup>

<sup>a</sup> Department of Geosciences, UiT – The Arctic University of Norway, PO Box 6050 Langnes, N-9037, Tromsø, Norway

<sup>b</sup> Department of Arctic Geology, University Centre in Svalbard, PO Box 156, N-9171, Longyearbyen, Norway

<sup>c</sup> Applied Petroleum Technology AS, PO Box 173 Kalbakken, N-0903, Oslo, Norway

<sup>d</sup> Equinor ASA, Harstad, Norway

<sup>e</sup> Department of Geosciences, University of Oslo, PO Box 1028 Blindern, N-0316, Oslo, Norway

<sup>f</sup> EP Skolithos, Sisikveien 36, 4022, Stavanger, Norway

### ARTICLE INFO

#### Keywords:

Svalbard  
Billefjorden group  
Røedvika formation  
Norwegian Barents shelf  
Source rock evaluation  
Depositional environment  
Coal

### ABSTRACT

Upper Palaeozoic strata are potential sources for hydrocarbon plays on the Norwegian Barents Shelf. The island of Bjørnøya (Bear Island) is located on the western margin of the Barents Shelf and represents an exposed part of the Stappen High, which makes it an excellent location to investigate the source rock potential of this succession. Here, we investigate the organic geochemical composition and source rock potential of coals and organic-rich mudstones of Late Devonian to middle Permian ages. The thermal maturity of the analysed samples ranges from mature to overmature with some samples being in the late oil generation window, and thus exhibiting higher maturities than age and facies equivalent strata in central Spitsbergen in the NW corner of the Barents Shelf and on the Finnmark Platform to the south. The high maturities and thermal cracking may thus have negatively affected the applied isoprenoid and biomarker-based source facies parameters, which potentially inhibit correct source facies interpretation. However, our results and comparisons with previous studies indicate that the vitrinite- and inertinite-dominated humic coals occurring in the lower part of the succession formed by the accumulation of peat in fluviially-influenced, humid wetlands at paleo-equatorial latitudes during a pronounced episode of rifting in the Late Devonian (Famennian) to earliest Carboniferous (Mississippian). Our source rock evaluation indicates a good potential for liquid hydrocarbon generation for the coals of the Upper Devonian Røedvika Formation prior to maturation. The oil-prone organic matter of these coals is primarily considered as terrestrial and non-aqueous. Because of renewed rifting in the middle Carboniferous combined with a shift to arid climatic conditions, as well as an environmental change from dominantly terrestrial and marginal marine clastic to marine carbonate platform environments, the accumulation of wetland peats effectively came to an end. Thus, the overlying Carboniferous and Permian strata generally seems to yield poor to no hydrocarbon generation potential.

### 1. Introduction

Upper Palaeozoic coals and organic-rich mudstones are inferred to be important source rocks on the Norwegian Barents Shelf, particularly in the under-explored northern and eastern areas (Grogan et al., 1999; van Koeverden et al., 2010, 2011; Norwegian Petroleum Directorate, 2017; Lutz et al., 2021). However, due to the sparsity of wells across this vast region, little is known about the lateral and stratigraphic distribution and generation potential of upper Palaeozoic source rock units (e.g.

Larssen et al., 2002; Larssen et al., 2005). Intriguingly, contributions from oils of Palaeozoic ages have been reported in exploration wells on the Loppa High at the western shelf margin (e.g. Ohm et al., 2008; Matapour et al., 2019), and exploration wells on the Finnmark Platform on the southern part of the shelf and onshore Spitsbergen at the uplifted northwest corner of the shelf, have established the petroleum potential of lower Carboniferous (Mississippian) coals (e.g. Abdullah et al., 1988; Nøttvedt et al., 1993; Bugge et al., 1995; Larssen et al., 2002, 2005; Senger et al., 2019; Olausen et al., 2023). On Spitsbergen, late

\* Corresponding author. Department of Geosciences, UiT – The Arctic University of Norway, PO Box 6050 Langnes, N-9037 Tromsø, Norway.  
E-mail address: [julian.janocha@uit.no](mailto:julian.janocha@uit.no) (J. Janocha).

<https://doi.org/10.1016/j.marpetgeo.2024.106768>

Received 9 October 2023; Received in revised form 24 January 2024; Accepted 19 February 2024

Available online 27 February 2024

0264-8172/© 2024 The Authors. Published by Elsevier Ltd. This is an open access article under the CC BY license (<http://creativecommons.org/licenses/by/4.0/>).

Carboniferous to early Permian-aged marine carbonates and interbedded shales also seems to hold some potential (e.g. Nicolaisen et al., 2018). Highly prolific marine carbonates are well known from the Upper Devonian on the Kara Shelf (e.g. Alsgaard, 1993; Petrov et al., 2008; Sobolev, 2018), whereas similar Devonian-aged source rock facies, do not occur on the Barents Shelf. In northern Spitsbergen, Devonian strata typically consist of continental red beds and yield an uncertain, but probably low potential for hydrocarbon generation (Blumenberg et al., 2018; Smelror et al., 2024). Upper Devonian (Famennian) to lower Carboniferous (Mississippian) coals and coaly shales on Bjørnøya at the western Barents Shelf margin may hold some highly uncertain generation potential (Bjørøy et al., 1980, 1983; van Koeverden et al., 2011), and Upper Devonian as well as upper Carboniferous lacustrine shales on the adjacent shelf margin, onshore East Greenland, reportedly yield some generation potential (e.g. Christiansen et al., 1990; Stemmerik et al., 1993).

Bjørnøya, the southernmost island of the Svalbard archipelago, lies strategically on the western margin of the Barents Shelf (Fig. 1A) and represents the rotated and exposed crest of the Stappen High. Here, a thick succession of upper Palaeozoic sedimentary rocks is excellently exposed (Fig. 1B and C). Because of its central position and its proximity to the Loppa High, which is an important area for exploration, Bjørnøya provides an important data point for understanding the distribution and potential of upper Palaeozoic source rocks on the Barents Shelf and adjacent basins.

The source rock potential of the upper Palaeozoic succession on Bjørnøya has only been addressed in a few publications, and several of these are based on very few samples spanning a limited part of the stratigraphy (Bjørøy et al., 1980, 1983; Abdullah et al., 1988; Michelsen and Khorasani, 1991; van Koeverden et al., 2011; Nicolaisen et al.,

2018).

In this paper, we provide organic geochemistry and source rock evaluation of coals, coaly shales and organic-rich mudstones from Bjørnøya spanning Upper Devonian to middle Permian strata (Fig. 1C). Our main objective is to establish and compare the source rock potential of these various organic-rich units, interpret the depositional conditions under which they accumulated, and discuss their development and maturity in relation to the geological history of the Stappen High and nearby basins. Although our dataset spans a wide range of stratigraphic intervals, we focus particularly on the Upper Devonian (Famennian) strata, as this interval are known to contain thick coals on Bjørnøya (Gjelberg, 1978, 1981; Michelsen and Khorasani, 1991).

## 2. Geological setting

### 2.1. Structural framework

Following the Caledonian Orogeny, the Barents Shelf, including the Stappen High and Bjørnøya, experienced multiple episodes of tectonic extension (Smelror and Petrov, 2018). The earliest extensional structures are associated with the post-orogenic collapse of the Caledonides and form an asymmetric rift basin (Gudlaugsson et al., 1998). In the late Carboniferous, localised rifting formed halfgrabens, which formed along reactivated Caledonian lineaments and structural grain (Smelror and Petrov, 2018). This rifting event is thought to form the main structuring event, resulting later in the opening of the North Atlantic Ocean (Faleide et al., 1984; Gudlaugsson et al., 1998; Blaich et al., 2017; Ryseth et al., 2021). This phase of localized rifting was followed by regional thermal subsidence extending into the late Permian (Gudlaugsson et al., 1998; Worsley et al., 2001). On the southern Stappen High, the late

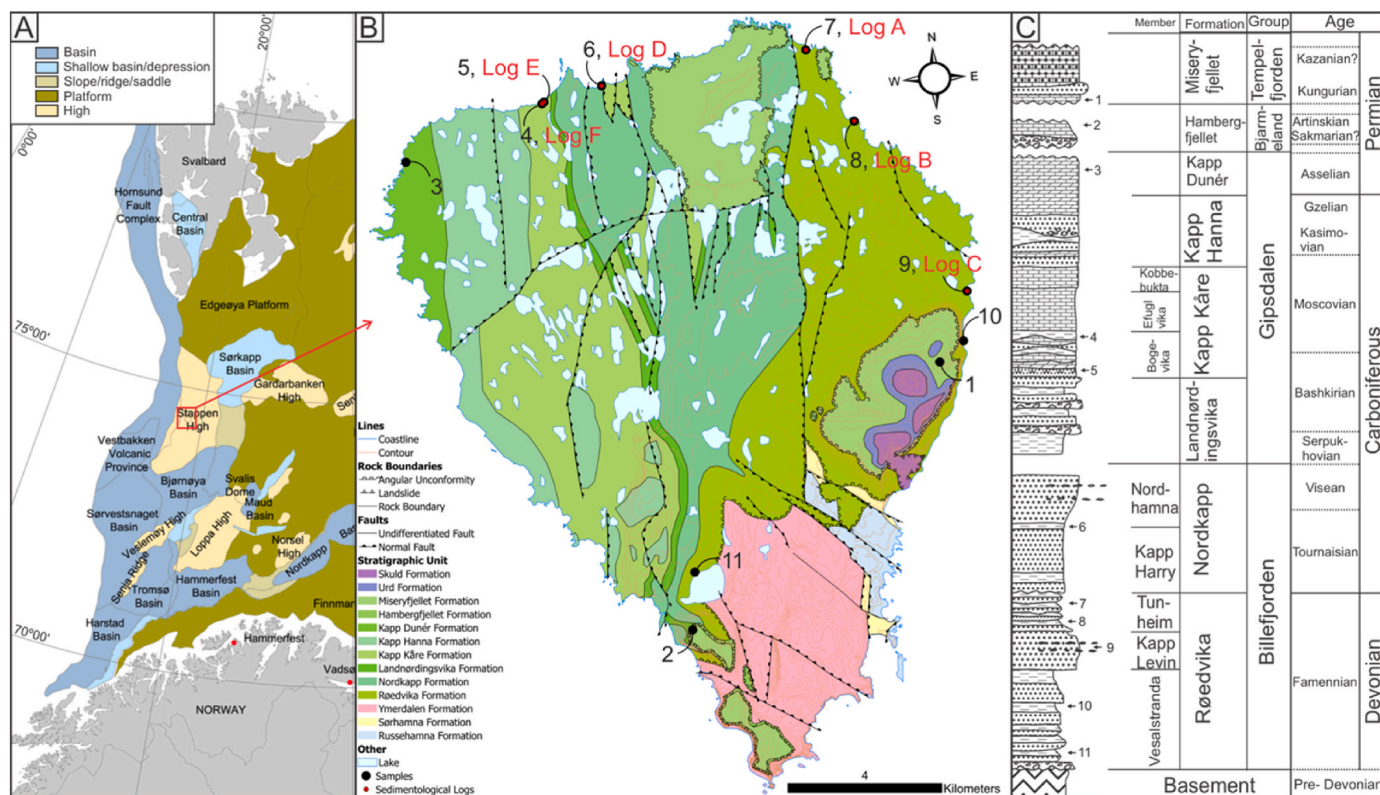


Fig. 1. Geographical overview of the studied area. (A) Structural Elements of the Western Barents Shelf between Svalbard and Norway. Modified after Henriksen et al. (2011). (B) Geological map of Bjørnøya with the sampling locations and stratigraphic sections shown in Fig. 5. Modified from Norwegian Polar Institute (2016). (C) Composite stratigraphic column of the upper Palaeozoic succession on Bjørnøya with indications of the sampled intervals. Modified from Worsley et al. (2001) and updated for the age of the Røedvika Formation from Lopes et al. (2021). Black numbers in B and C indicate the sampled intervals. 1: P7-8; 2: P32; 3: P1-2; 4: P70-71; 5: P68-69; 6: P62-65; 7: P41-43 & EP37-40; 8: P44-50 & EP41-47; 9: P52-54 & EP48-53; 10: P3-6 & EP11-16; 11: P30-31 & EP31-32.

Carboniferous faults were reactivated during renewed rifting in the late Permian–Early Triassic (Gudlaugsson et al., 1998; Blaich et al., 2017; Tsikalas et al., 2021). A subsequent phase of regional subsidence followed, lasting until renewed rifting in the Late Jurassic to Earliest Cretaceous once again reactivated pre-existing structures and formed horst and graben structures across the Stappen High (Faleide et al., 1984; Blaich et al., 2017).

The upper Palaeozoic succession consists of mixed clastic and carbonate sedimentary rocks and is up to 1.2 km thick (Ritter et al., 1996; Worsley et al., 2001; Tsikalas et al., 2021). Internally, the succession exhibits multiple unconformities which can be attributed to recurrent fault-related uplift and tilting events that took place particularly during the Carboniferous and Permian (e.g. Gjelberg, 1981; Gjelberg and Steel, 1981; Worsley et al., 2001; Tsikalas et al., 2021; Grundvåg et al., 2023). The most prominent angular unconformity separates Devonian–Carboniferous strata from Permian (Worsley et al., 2001; Grundvåg et al., 2023). Onwards from the middle Permian until the Late Cretaceous, the Stappen High and Bjørnøya experienced high rates of thermally driven subsidence accompanied by high sedimentation rates. The upper Palaeozoic succession was therefore deeply buried, in the order of several kilometres (Ritter et al., 1996). Onwards from the Late Cretaceous, approximately 3–4 km of overburden have subsequently been removed from Bjørnøya (Fig. 2, Ritter et al., 1996), possibly with as much as 2 km removed only during the Cenozoic (Laberg et al., 2012; Lasabuda et al., 2018, 2021).

## 2.2. Lithostratigraphy and depositional environments

During the late Palaeozoic, Bjørnøya and Svalbard drifted northwards from c. 10°N in the Late Devonian to c. 40°N in the late Permian (Smelror et al., 2009; Golonka, 2020). This northward drift across several climatic zones in combination with regional structuring events and relative sea-level changes driven by local fault movements and glacio-eustasy (caused by waxing and waning of the Gondwana ice sheet) is all reflected in the stratigraphic rock record (e.g. Stemmerik, 1997).

The Upper Devonian to lower Carboniferous Billefjorden Group is dominated by various terrestrial clastics of the Røedvika and Nordkapp formations. These units were deposited in an elongated WNW–ESE-oriented fault-bounded basin (Fig. 3A, Horn and Orvin, 1928; Worsley and Edwards, 1976; Gjelberg, 1978, 1981; Worsley et al., 2001). The frequent occurrence of coals in this part of the succession indicates that warm and humid climatic conditions prevailed, and the intercalation of coarse-grained clastics, presumably derived from footwall erosion, and mudstone-dominated units, suggests that recurrent extensional fault-activity had a major control on deposition (e.g. Gjelberg, 1981; Gjelberg and Steel, 1981).

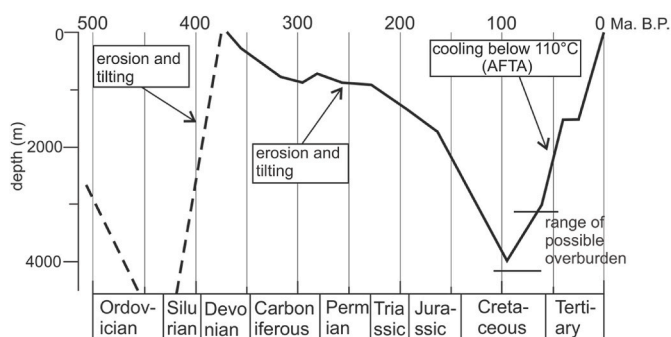


Fig. 2. Burial and erosion history of Bjørnøya. Graph shows the maximal burial depth calculated from the maximum burial temperature derived from apatite fission track analysis, vitrinite reflectance and fluid inclusions and paleogeothermal gradient. Modified after Ritter et al. (1996) and Worsley et al. (2001).

The Upper Devonian (Famennian) Røedvika Formation (Lopes et al., 2021) is divided into several Members recording deposition in various alluvial environments, including flood plains transected by meandering channel belts (i.e., the Vesalstranda Member, Fig. 3E), braided rivers and lacustrine deltas (i.e., the Kapp Levin Member, Fig. 3F), and low-sinuosity meandering channel belts (i.e., the Tunheim Member; Fig. 3G–Worsley and Edwards, 1976). The Tunheim Member is known for containing several coal seams which were subject to commercial interest in the early part of the 20th century (Horn and Orvin, 1928).

The lower Carboniferous (Mississippian) Nordkapp Formation (Viséan; Kaiser, 1970) is subdivided into the Kapp Harry and the Nordhamna Members (Gjelberg, 1981; Dallmann, 1999), collectively recording deposition in a braid plain setting (Fig. 1C). Thin coals occur in the Nordhamna Member, possibly reflecting the accumulation of plant debris and peat in abandoned channel belts or transient intra-channel flood plains (Fig. 3H–Gjelberg, 1981).

Renewed rifting in the middle Carboniferous resulted in the formation of several localized rift basins across the Barents Shelf including the inferred Bjørnøya Trough and the renowned Billefjorden Trough in Spitsbergen (Fig. 3C–Gjelberg and Steel, 1981; Johannessen and Steel, 1992; Smyrak-Sikora et al., 2018). The syn- to early post-rift infill of these basins is assigned to the upper Carboniferous to lower Permian Gipsdalen Group (Worsley et al., 2001). A drastic change from humid to arid climate occurred in the early to middle Carboniferous and is recorded as terrestrial red beds in the Landnørdingsvika Formation in the lower part of the Gipsdalen Group on Bjørnøya (Gjelberg, 1981; Gjelberg and Steel, 1981; Worsley et al., 2001). These red beds record the interfingering and accumulation of floodplain, marginal marine, and alluvial fan deposits in an active, fault-controlled basin under arid climatic conditions (Gjelberg, 1981; Gjelberg and Steel, 1981; Worsley et al., 2001).

A regional transgression during the Bashkirian to Moscovian promoted a shift to marine depositional environments and deposition of the carbonate dominated Kapp Kåre Formation, which is divided into the Bogeivika, Eflugvika and Kobbebukta Members (Fig. 1C–Worsley and Edwards, 1976). The Bogeivika Member, which is a mixed clastic and carbonate unit, contains multiple upwards-coarsening sequences which record successive shoreline progradation's and basin shallowing governed by high frequency, glacio-eustatically driven relative sea-level fluctuations (Fig. 1C–Stemmerik and Worsley, 2000; Worsley et al., 2001). The sandstone content decreases upwards in the unit, marking a transition into the open-marine limestones of the Eflugvika Member. By the end of the Carboniferous, a regionally extensive carbonate platform was eventually established (Fig. 3D–Stemmerik and Worsley, 2000; Worsley et al., 2001). However, periods of uplift, subaerial exposure and karst development occurred frequently, particularly on the Stappen and Loppa highs. The Kapp Hanna Formation (not considered here) records the accumulation of paralic deposits in very localized basins which formed during renewed fault activity in the latest Carboniferous (Worsley et al., 2001).

The overlying carbonates of the Kapp Dunér Formation (Gzhelian–Asselian) were deposited in shallow marine and lagoonal, as well as reef and intra-reef settings and were part of a regionally extensive warm-water carbonate platform (Stemmerik, 1997; Worsley et al., 2001). The top of the unit is marked by a distinct karst surface, indicating uplift and prolonged exposure of the platform.

Warm to cool-water carbonates of the lower to middle Permian Hambergfjellet Formation (late Asselian–late Artinskian) of the Bjarmeland Group, was deposited during a regional transgression which eventually drowned most of the Stappen High (Stemmerik, 1997; Worsley et al., 2001; Grundvåg et al., 2023). The fossil fauna indicates warm water and restricted conditions for the lower part of the unit and open marine, cool water conditions for the upper part of the unit (Grundvåg et al., 2023). In addition, there are several indications of frequent episodes of subaerial exposure, minor fault activity, and recurrent tilting of the succession, presumably reflecting fault activity

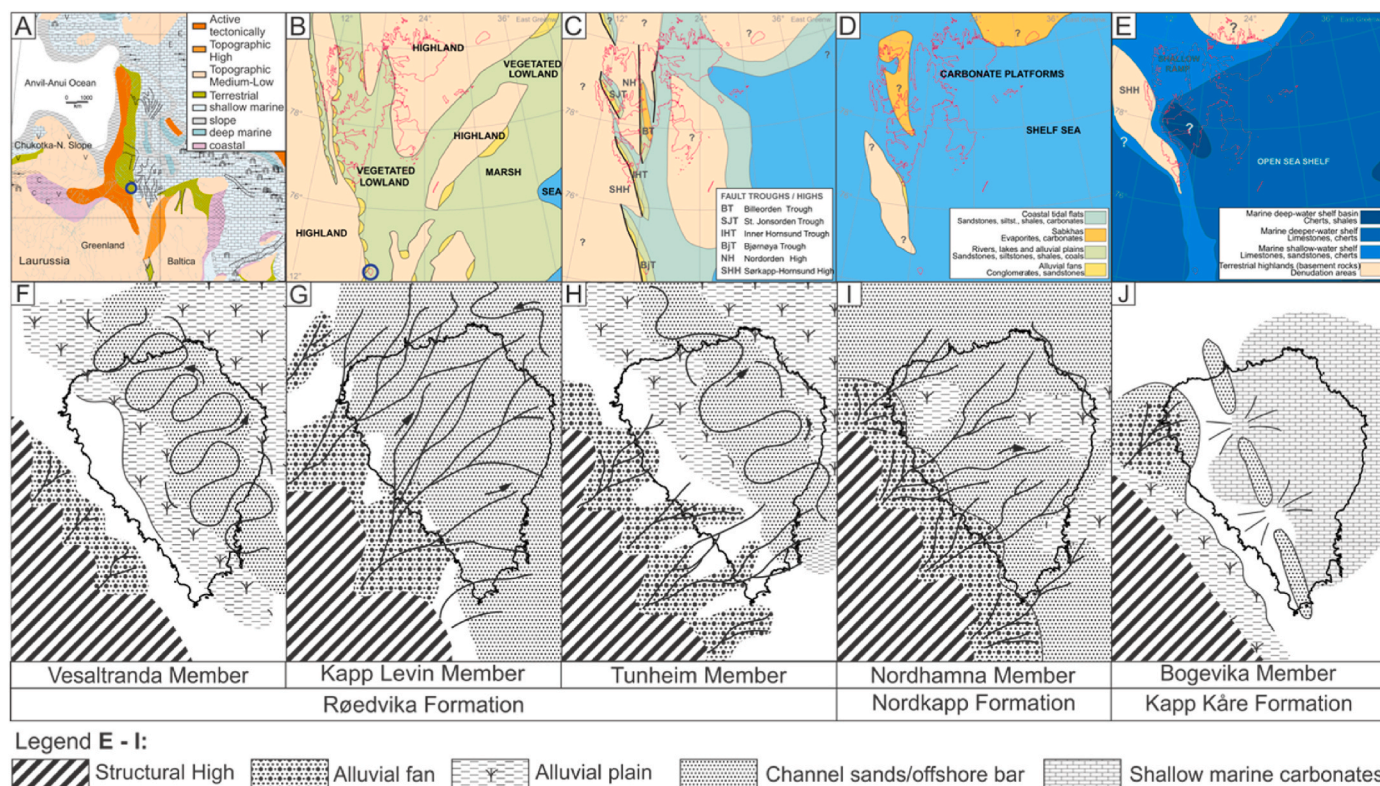


**Fig. 3.** Palaeogeographical reconstructions and inferred depositional environments for: (A) The Late Devonian at 370 Ma during the Famennian. Blue circle shows the approximate location of Bjørnøya. Modified after Golonka (2020) (B) The Early Carboniferous during the Viséan at approximately 340 Ma (i.e., during deposition of the Nordkapp Formation, Billefjorden Group). Blue circle highlights the location of Bjørnøya (C) The late Carboniferous during the Bashkirian at approximately 320 Ma (i.e., during deposition of the Landnørdingsvika Formation, lowermost Gipsdalen Group). (D) The late Carboniferous at approximately 300 Ma during the Gzhelian (i.e., during deposition of the Kapp Kåre Formation, Gipsdalen Group). (E) Late Permian at around 265 Ma during the Guadalupian. B – E modified after Dallmann et al. (2019). (F) Palaeogeographical reconstruction of the meandering stream deposits of the Vesalstranda Member. (G) Palaeogeographical reconstruction of the braided stream depositional environment of the Kapp Levin Member. (H) Palaeogeographical reconstruction of the meandering stream depositional environment of the Tunheim Member. (I) Palaeogeographical reconstruction of the braided stream depositional environment of the Nordhamna Member. F – J modified after Gjelberg (1981) (J) Palaeogeographical reconstruction of the shallow marine depositional environment of the Bogeвика Member. Modified after Worsley et al. (2001).

along the western part of the Stappen High (Worsley et al., 2001; Grundvåg et al., 2023).

The overlying cool-water carbonates of the middle to upper Permian Miseryfjellet Formation (Kungurian–Wordian) of the Tempelfjorden Group (Worsley and Edwards, 1976) marks the final drowning of the Stappen High and the establishment of a circum-Arctic, cool-water carbonate platform that persisted until the earliest Triassic (Fig. 3D–Stemmerik, 1997).

### 3. Methods

Sampling was undertaken for the bulk of the Palaeozoic succession of Bjørnøya, spanning the Upper Devonian to lower Carboniferous Billefjorden Group, the upper Carboniferous to lower Permian Gipsdalen Group, the lower to middle Permian Bjarmeland Group, and the middle Permian Tempelfjorden Group. Units characterized by organic-lean siltstones and continental red beds were also sampled (e.g., the Kapp Hanna and Landnørdingsvika formations), but have not been analysed due to the generally low petroleum generating potential of such lithologies. The sampling locations are shown in Fig. 1B and a brief sample description is given in Table 1. The sample set consists of 58 samples of various lithologies and formations including siltstones ( $n = 12$ ), coals ( $n = 14$ ), shales ( $n = 15$ ), coaly shales ( $n = 8$ ), calcareous shales ( $n = 1$ ) and siliceous shales ( $n = 3$ ). The sample set include samples from two merged sample sets that both were collected by personnel from UiT – The Arctic University of Norway (UiT) and Equinor ASA during a

common field campaign in 2016.

The UiT sample set (samples annotated with P followed by a number) was analysed by Applied Petroleum Technology (APT) in Oslo, Norway, and the Equinor sample (samples annotated with EP followed by a number) set at the Equinor in-house lab in the Sandsli office, Bergen, Norway. An overview of the various analytical methods applied is provided in Table 1, and a detailed method description for both laboratories is available as supplementary material. All the analytical procedures follow standard applications and comply with the specifications given in the Norwegian Industry Guide on Organic Geochemical Analyses (NIGOGA; Weiss et al., 2000).

### 4. Results

Selected outcrop locations where the Upper Devonian Røedvika Formation samples were collected are shown in Fig. 4, and accompanying sedimentological logs of the investigated outcrop sections are shown in Fig. 5 to provide stratigraphic context.

#### 4.1. TOC and Rock-Eval pyrolysis

Analytical results from total organic carbon (TOC) measurements and Rock-Eval screening are given in the supplementary material and shown in Fig. 6. The samples show a large spread in TOC, ranging from 0.08 wt% in the siltstones of the Røedvika Formation to a maximum value of 86.85 wt % in a coal sample of the same formation. Note that all

Table 1

Complete list of analysed samples. The various analytical programs are grouped in to three groups: G1, G2 and G3. Analyses performed for each group are as follows: G1: TOC and Rock-Eval. G2: Solvent extraction, Iatroscan, Asphaltenes, GC-FID chromatography and for all x\* stable isotopes in addition. G3: GC-MS chromatography. VR: Vitrinite reflectance.

Sample No.	Outcrop	GPS Location (UTM 33X)		Formation	Member	Age	Lithology	Depositional environment	References	Depth in MDP [m]	G1	G2	G3	VR									
P1	Amfiet	612785	8269932	Kapp Dunér	Upper part of the Unit	E. Permian	Shale	Warm water carbonate shelf - inter reef facies	General description given in Worsley et al. (2001) p.25 (p. 219 of that volume).		x												
P2											x												
P3	Vesalstranda	627217	8265272	Røedvika	Vesalstranda	L. Devonian	Coal	Flood plain adjacent to meandering channels	General description given in Gjelberg (1981) p.9, samples collected in section 3 in his Fig. 4.	195	x												
P4							201			x	x*	x	x										
P5							211			x			x										
P6							212,6			x	x*												
EP11							190,1			x	x	x											
EP12							190,2			x													
EP13							190,3			x	x	x											
EP14							190,4			x													
EP15							190,6			x	x	x											
EP16							191,2			x	x	x											
P7	Brettingsdalen	626620	8264753	Miseryfjellet	Few m above base	L. Permian	Siliceous	Open marine cold water carbonate shelf	General description given in Worsley et al. (2001) p.28 (222 of that volume).		x												
P8							Shale				x												
P30	Ellasjøen	620271	8259289	Røedvika	Vesalstranda	L. Devonian	Shale	Flood plain between channels	General description given by Gjelberg (1981). Based on map by Dallmann and Krasil'Shchikov (1996), these samples are collected from the Vesalstranda Mb.	30	x	x*		x									
P31							Shale			30,5	x			x									
EP31							Shale			30,75	x	x*	x										
EP32							Siltstone			31,25	x												
P32	Alfredfjellet W Titrebekkyttane	620216	8257790	Hamborgfjellet Røedvika	Upper part of unit Tunheim (upper part)	E. Permian	Siliceous shale	Open marine, warm-cool water carbonate shelf	General description in Worsley et al. (2001) p.26 (p.220 in volume)		x												
P41							Coal				341,6	x	x*	x	x								
P42							Siltstone				341,8	x											
P43							Shale				344,8	x	x*		x								
EP37							Coal				341,65	x	x	x									
EP38							Shale				341,75	x											
EP39							Shale				343	x											
EP40							Shale				344,75	x											
P44							Jacobsenodden				624409	8270988	Røedvika	Tunheim (Lower part)	L. Devonian	Coal	Flood plain between meandering channels	The A-coal + strata below. This is the lower part of the upper unit of the Tunheim Mb, see Mørk et al. (2014) p.18. Samples from their profile S in F. 24.	325,6	x	x*	x	
P46																Shale			329,5	x			
P47	Coaly shale	332	x	x*		x																	
P48	Shale	333,5	x																				
P49-0	Coaly shale	335,5	x																				
P49-1	Coal	335	x																				
P49-2	Coal	336	x	x*	x	x																	
P50	Siltstone	336,8	x	x*	x																		
EP41	Siltstone	325,3	x																				
EP42	Coal	323,5	x	x	x																		
EP43	Silty shale	329	x																				
EP44	Coal	334,8	x																				
EP45	Shale	336,1	x	x	x																		
EP46	Sandstone	338	x																				
EP47	Sandstone	337,5	x																				
P52	Kapp Levin	627325	8266596	Røedvika	Kapp Levin (Upper shale)	L. Devonian	Siltstone	Lacustrine	Facies association KD of Gjelberg (1981), see his Fig. 9 (and uppermost 15 m of his Fig. 5A).	286,3	x												
P53							Siltstone			287,55	x												
P54							Siltstone			289,3	x												
EP48		627298	8266712		Kapp Levin		Sandstone	Channel fill		298,3	x												
EP49							Sandstone			296,4	x	x*	x										
EP50		627325	8266596		Vesalstranda		Siltstone	Flood plain	General description in Gjelberg (1981).	286	x	x*	x										

(continued on next page)



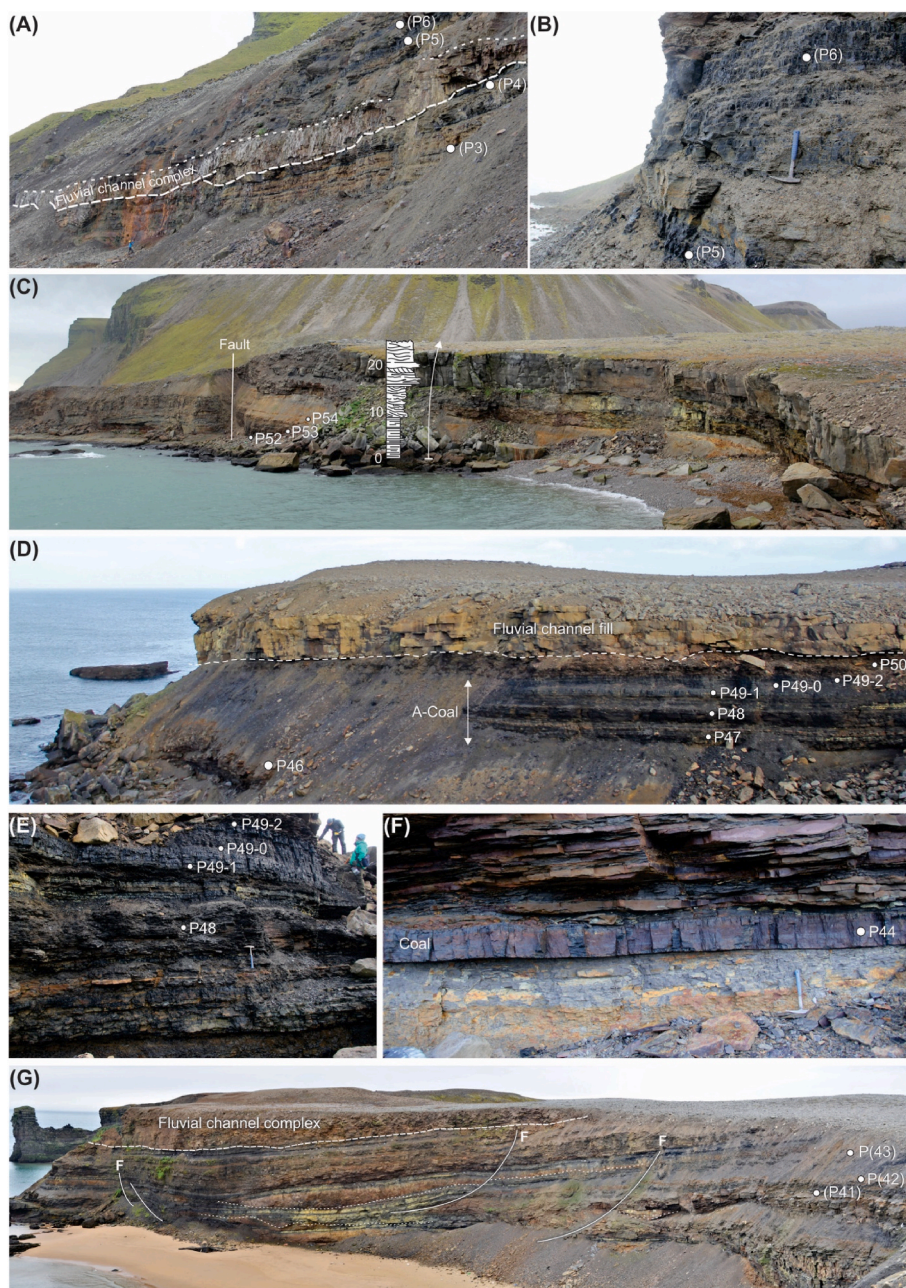


**Fig. 4.** Outcrop images showing the location of the samples collected in the Upper Devonian Røedvika Formation. **(A)** Coal sample locations P3 – P6 of the upper Vesalstranda Member in Brettingsdalen. Person for scale in the lower left. **(B)** Close-up of some of sampling locations P5 and P6 in the upper part of the Vesalstranda Member in Brettingsdalen. Hammer for scale. **(C)** Siltstone sampling locations P52 and P53 in the upper part of the Kapp Levin Member at Kapp Levin. Sedimentary log from Gjelberg (1981) showing the coarsening upwards unit in the upper part of the member, possibly representing a lacustrine delta system. Log for scale. **(D)** Sampling locations P46 – P50 of the A-Coal seam of the lower Tunheim Member at Jacobsenodden. **(E)** Close up of sampling locations P48 – P49-2 of the A-Coal seam at Jacobsenodden. Hammer for scale. **(F)** Sample P44 of the Lower Tunheim Member below the A-Coal seam at Jacobsenodden. Hammer for scale. **(G)** Sampling locations P41 – P43 of the upper part of the Tunheim Member at Titrebekkpyttane.

#### 4.3. Molecular geochemistry and stable carbon isotope analyses

The gas chromatography coupled with flame ionization detection (GC-FID) of the rock extracts are shown in Fig. 8. The medium hydrocarbon range ( $C_9$ – $C_{19}$ ) is the most abundant saturate fraction, resulting in a waxiness ratio ranging from 0.64 to 0.93 (using the waxiness ratio  $n-C_{17}/(n-C_{17}+n-C_{27})$ ; Justwan et al., 2006). Most samples show a negligible abundance of unresolved complex mixture (UCM), and arguably exhibit a unimodal n-alkane distribution. The alkanes  $n-C_{17}$  and  $n-C_{18}$  are generally far more abundant than their related isoprenoids Pristane (Pr) and Phytane (Ph), resulting in Pr/ $n-C_{17}$  and Pr/ $n-C_{18}$  ratios

<1 for all but two samples (Fig. 9A). Mixed marine – transitional terrigenous organic matter is suggested by the Pr/ $n-C_{17}$  and Pr/ $n-C_{18}$  ratios. Pristane/Phytane ratios range between 0.84 and 2.88 and are inconclusive with respect to their depositional environment (Peters et al., 2005a).

Typical  $m/z$  191 terpane fragmentograms of the Røedvika Formation samples are shown in (Fig. 10). In general, all gas chromatography mass spectrometry (GC-MS) fragmentograms show a low signal to noise ratio and are therefore considered to be of questionable quality. Nevertheless, variable concentrations in  $C_{19}$ – $C_{24}$  tricyclic terpanes are detected, resulting in ( $C_{19}$ – $C_{24}$ ) tricyclics/30 $\alpha$ B ratios ranging from 5.63 to 16.82.

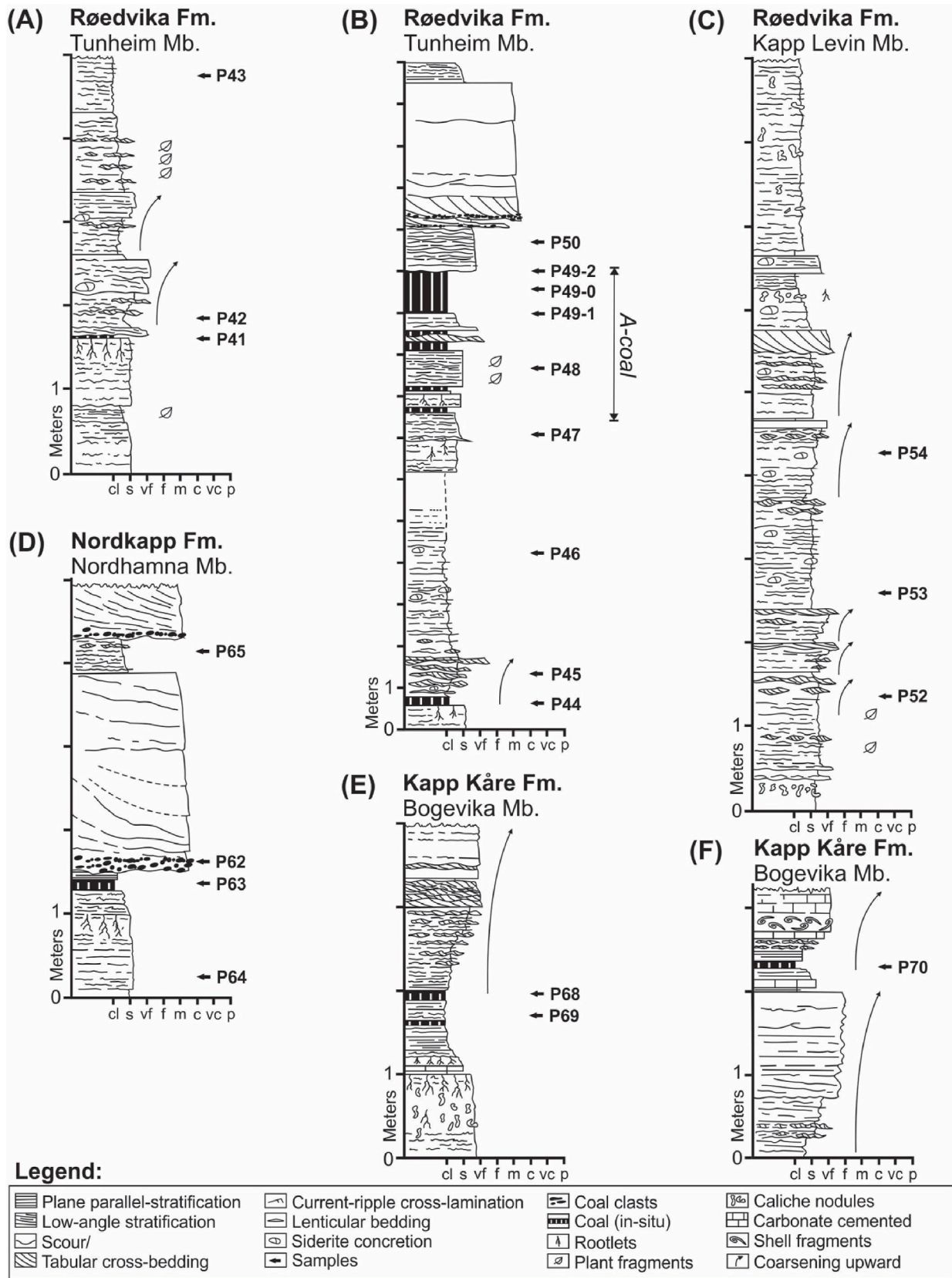


**Fig. 5.** Sedimentological logs of key locations on Bjørnøya documenting the sedimentology and stratigraphy for some selected sample intervals. (A) Log through parts of the upper part of the Tunheim Member of the Rødsvika Formation at Titrebeekpyttane showing sample locations P41 – P42. (B) Log through the lower parts of the Tunheim Member of the Rødsvika Formation at Jacobsenodden showing sample locations P44 – P50. (C) Log through the upper part of the Kapp Levin Member of the Rødsvika Formation at Kapp Levin showing sample locations P52 – P54. (D) Log through the lower Nordhamna Member of the Nordkapp Formation at Nordhamna showing sample locations P62 – 65. (E) Log through part of the lower Bogeivika Member of the Kapp Kåre Formation in Kobbbebukta showing sample locations P68 – P69. (F) Log through the upper Bogeivika Member of the Kapp Kåre Formation in Kobbbebukta showing sample location P70.

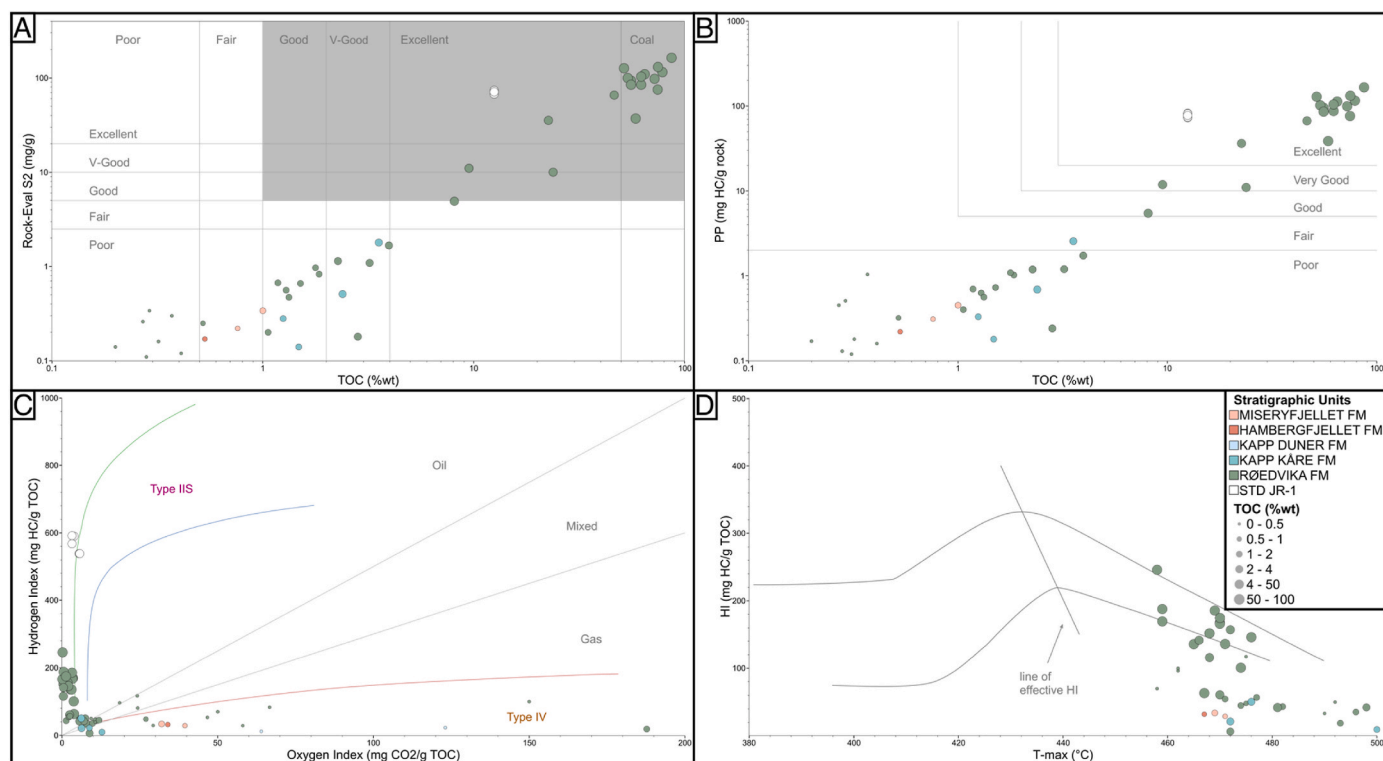


**Fig. 6.** Scatter plots of selected Rock-Eval parameters. **(A)** S2 (mg HC/g rock) vs. TOC (%). The solid grey lines and the dashed black lines infer hydrogen index (HI), following Peters and Cassa (1994). **(B)** Petroleum Potential (PP) vs. TOC %wt. **(C)** Modified Van Krevelen diagram based on Hydrogen index (HI) (mg HC/g TOC) vs. Oxygen Index (OI) (mg CO<sub>2</sub>/g TOC). The solid-coloured lines infer the maturation pathways of the respective kerogen Type, and the fields separated by dashed black lines infer the resulting petroleum product at peak maturity, following Dembicki (2009). Type IV kerogen is regarded as inert and without any hydrocarbon potential.  $HI = (S2/TOC) * 100$ ;  $OI = (S3/TOC) * 100$  **(D)** Cross plot of HI vs. T<sub>max</sub> showing the line of effective HI. Graph based on Sykes and Snowdon (2002). Lithostratigraphic colours for plots A-D after the NPD Geostandard (Norwegian Petroleum Directorate, 2022).

The C<sub>24</sub> tetracyclic terpane is readily identified, while the C<sub>25</sub>–C<sub>30</sub> tricyclic terpanes are generally absent or indistinct. Of the defined C<sub>29+</sub> hopenes, the norhopane (29αβ), diahopane (30d) or hopane (30αβ) are the most abundant. However, some of the data is of questionable quality due to low signal-to-noise ratio. The m/z 217 and m/z 218 fragmentograms of the sterane biomarker show even less biomarker concentrations. Thus, sterane biomarker ratios are not considered in further discussions.

The extractable organic matter (EOMs) of the Røedvika Formation show abundant aromatic hydrocarbons in the m/z 142 (methyl-naphthalenes), m/z 159 (dimethylnaphthalenes), m/z 178 (phenanthrene), m/z 192 (methylphenanthrenes), m/z 206 (dimethylphenanthrenes), m/z 184 (dibenzothiophene), and m/z 212 (methyl-dibenzothiophenes) fragmentograms, while m/z 170 (trimethylnaphthalenes) show lower concentrations. Representative fragmentograms of the aromatic fraction of the Røedvika Formation extracts are displayed in Fig. (11). Dimethylnaphthalene ratios (DMNR; Alexander et al., 1983; 1985) range from 4.98 in sample EP49 from the Kapp Levin Member to 20.08 in sample P50 from the Tunheim Member at the Jacobsenodden locality. Related vitrinite reflectance (%R<sub>c</sub>(DMNR-1)) was calculated to be 0.9 to 2.3%R<sub>c</sub>(DMNR-1), respectively (Alexander et al., 1983). Radke et al. (1982a), (1982b) and Radke and Welte (1983) observed a maturity relationship between methylphenanthrenes. The methylphenanthrene ratio (MPR) vary between 1.82 in sample EP45 and 3.41 in sample P41 in the Tunheim (at the Jacobsenodden locality) and Vesalstranda Members, respectively. The calculated reflectance in the before-mentioned samples is 1.20 and 1.47 %R<sub>c</sub>(MPR). The methylphenanthrene indices (MPI-1) range from 0.95 (P50, Jacobsenodden locality) to 1.56 (EP49, Kapp Levin locality) with a calculated reflectance of 0.97 and 1.34 %R<sub>c</sub>(MPI-1), for MPI-1 < 1.35 %R. The %R<sub>c</sub> rises to 1.73 and 1.36 %R<sub>c</sub>(MPI-1) for MPI-1 > 1.35 %R. Dibenzothiophene to

phenanthrene (DBT/PHEN) ratios are low with ratios of 0.02–0.08, in samples EP42 and EP37 of the Tunheim Member at the Jacobsenodden and Titrebekkpyttane localities, respectively (see Fig. 1 for sample locations).

The δ<sup>13</sup>C isotope composition of the saturate and aromatic fractions show a large spread with values ranging from –31.20 to –24.50 ‰ and –24.90 to –22.10 ‰, respectively. Most samples plot in an area being indicative for non-marine organic matter (Fig. 9B), which is also suggested from the Canonical Variable (Sofer, 1984) as shown in Fig. 9C.

## 5. Discussion

Based on the Rock-Eval results, vitrinite reflectance measurements, and the subsequent organic geochemical analyses, the following discussion will only focus on the maturity, source facies and petroleum potential of the coal-bearing deposits of the Upper Devonian (Famenian) Røedvika Formation (i.e. the Vesalstranda and Tunheim Members, Fig. 1C).

### 5.1. Maturity

The maturity of some upper Palaeozoic strata on Svalbard has been assessed in previous studies (Bjørøy et al., 1980, 1983; Michelsen and Khorasani, 1991; van Koeverden et al., 2011; Nicolaisen et al., 2018). Bjørøy et al. (1983), which focused on the Devonian succession of Bjørnøya, suggests a slightly higher maturity in the Devonian succession (1.3–1.5 %R<sub>m</sub>) in the centre of the island and lower maturities, ranging from 0.9 to 1.2 %R<sub>m</sub>, on the western and eastern sides. Ritter et al. (1996) on the other hand report increasing maturities from south (1, 02–1,46%R<sub>m</sub>) to north (1,26–1,75%R<sub>m</sub>). Our sample set comprises too scattered and too few vitrinite reflectance measurements, to record the

**Table 2**

Sub-sample set with visual maceral analysis. %Ro: measured vitrinite reflectance; SD: standard deviation. The comments on the organic petrography are based on the original geochemical report by APT.

Sample	Stratigraphic unit	Facies	%Ro ± SD	Comments on organic petrography
P4	Vesalstranda Mb.	Coal	1.10 ± 0.07	100 % telinite. Yellow & yellow orange fluorescing blebs in voids. Live hydrocarbons observed.
P5	Vesalstranda Mb.	Coal	1.25 ± 0.07	100 % collinite, but a hint of cell structure is sometimes present. Reddish-orange fluorescing wisps and blebs.
P30	Vesalstranda Mb.	Shale	1.58 ± 0.13	100% collinite, generally in rough laminae along bedding. Orange-brown fluorescing matrix, and reddish-orange wisps and blebs, probably not exinite.
P31	Vesalstranda Mb	Shale	1.43 ± 0.10	Wispy vitrinite in argillaceous fabric and collinite in coaly clasts. Vitrinite merges with semifusinite. Reddish-orange fluorescing liptodetrinite.
P41	Tunheim Mb.	Coal	1.22 ± 0.08	Mostly telinite. Cellular structure more apparent than in P4. Reddish-brown fluorescing laminae and blebs, probably from hydrocarbons in fractures.
P43	Tunheim Mb.	Shale	2.20 ± 0.20	Vitrinite and inertinite fragments common, with overlapping reflectivities. Inertinite tends to be more angular. No fluorescing macerals.
P47	Tunheim Mb.	Coaly shale	1.23 ± 0.08	Argillaceous coal perhaps containing lamalginite. Vitrinite most often seen as telinitic laminae. Some inertinite present. Reddish-brown fluorescing matrix.
P49-2	Tunheim Mb.	Coal	1.32 ± 0.08	Trimacerite with common vitrinite and inertinite, while exinite is less common. Yellow fluorescing void filling blebs.

suggested maturity differences. Measured vitrinite reflectance in the Vesalstranda and Tunheim Members, ranging between 1.1 and 1.58 % Rm, show slightly higher maximum value than the values reported by Bjørøy et al. (1983) (Fig. 12G). Jarvie (2018) and Evenick (2021) presented a correlation between measured T<sub>max</sub> values and vitrinite reflectance of shales. For our dataset, we find that T<sub>max</sub> and vitrinite

reflectance correlate well using the (Jarvie, 2018) calculation (Fig. 13). Thus, %Rc(T<sub>max</sub>) may add useful vitrinite reflectance equivalent maturity data where vitrinite reflectance measurements are missing (Fig. 12H and I).

The highest T<sub>max</sub> measurements and thus highest calculated %Rc (T<sub>max</sub>) values are found in the low TOC samples, in both the Vesalstranda, Kapp Levin, and Tunheim Members (Fig. 12D–H,I). These significantly higher T<sub>max</sub> values can be related to organic matter oxidation, as all our samples are surface samples from coastal cliff sections currently experiencing high rates of erosion. Thus, we consider our coal samples as pristine.

In addition to vitrinite reflectance and Rock-Eval T<sub>max</sub>, we used the methylphenanthrene ratio (MPR) and the dimethylnaphthalenes ratios (DMNR1) measurements to calculate the vitrinite reflectance (Fig. 12J and K, Radke et al., 1982b; Alexander et al., 1983, 1984, 1985; Kvalheim et al., 1987; Radke, 1988). The calculated %Rc(DMNR-1) appears to be slightly higher than the measured vitrinite reflectance (%Rm), while the %Rc(MPR) fit our measured Rm quite well (Fig. 12G–J,K). In general, our dataset shows that the samples are late mature to postmature with respect to oil generation (Peters and Cassa, 1994), but may be in the main gas generation window (1.3–2.2% Rm; see Cornford, 1998). This coincides with vitrinite reflectance measurements obtained by previous studies (Bjørøy et al., 1980, 1983; Michelsen and Khorasani, 1991; Ritter et al., 1996). Similar to Wesenlund et al. (2021) we find that the maturities appear to be at least partly dependent on their lithofacies, based on the calculated vitrinite reflectance's. Sandstones appear to have a slightly lower maturity than coal while coaly shales, shales and siltstones appear to have a slightly higher maturity. Previous studies report vitrinite reflectance values between 0.6 and 1.0%Rm for coals in central Spitsbergen (Abdullah et al., 1988; Michelsen and Khorasani, 1991; van Koeverden et al., 2011; Nicolaisen et al., 2018), and between 0.62 and 1.1%Rm from coals on the Finnmark Platform (van Koeverden et al., 2010). Thus, comparing measured vitrinite reflectance values of the coals on Bjørnøya with lower Carboniferous coals from Central Spitsbergen and from the Finnmark Platform, shows that the Upper Devonian coals of Bjørnøya exhibit higher maturities. The elevated vitrinite reflectance values on Bjørnøya can either be explained by an elevated geothermal gradient after deposition of the stratigraphic intervals in question or because of deep burial. Previous studies have not reported an increased or anomalous geothermal gradient for Bjørnøya or the SW Barents Shelf (Ritter et al., 1996; Ohm et al., 2008; Smelror et al., 2009). However, several studies have shown that the western Barents Shelf comprises a thick Triassic and Cretaceous cover (Gudlaugsson et al., 1998; Faleide et al., 2008; Blaich et al., 2017; Hagset et al., 2022). Furthermore, basin modelling has shown that the western Barents Shelf experienced deeper burial than the eastern and northern parts (Gac et al., 2018; Lutz et al., 2021). Vitrinite reflectance of more than 1,1%

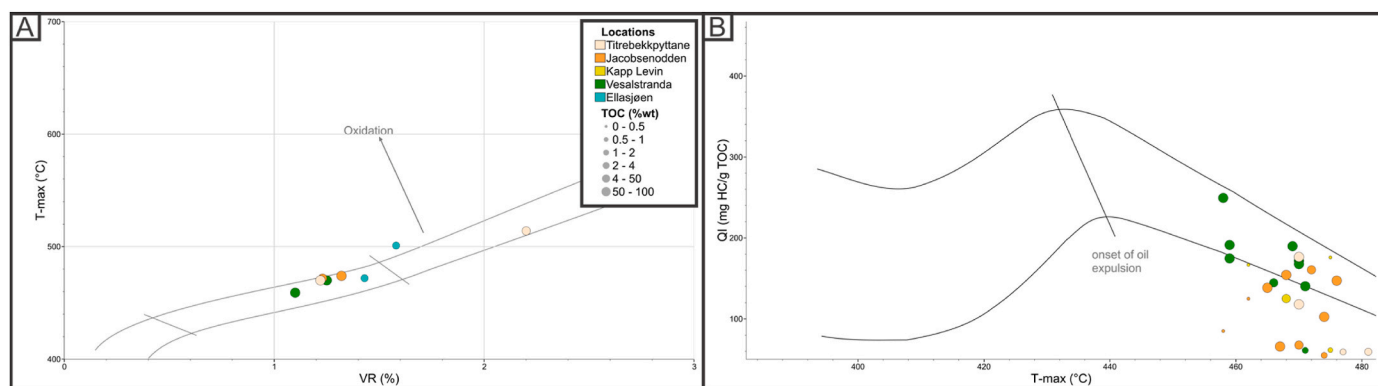


**Fig. 7.** (A) Cross plot of vitrinite reflectance over T<sub>max</sub> after Teichmüller and Durand (1983). Legend is for scatter plots A&B. Size of circles is based on TOC while colour corresponds to sampling location. (B) Cross-plot of quality index (QI) [(S1+S2)/TOC] against T<sub>max</sub>, and the inferred rank thresholds for oil expulsion after Sykes and Snowdon (2002).

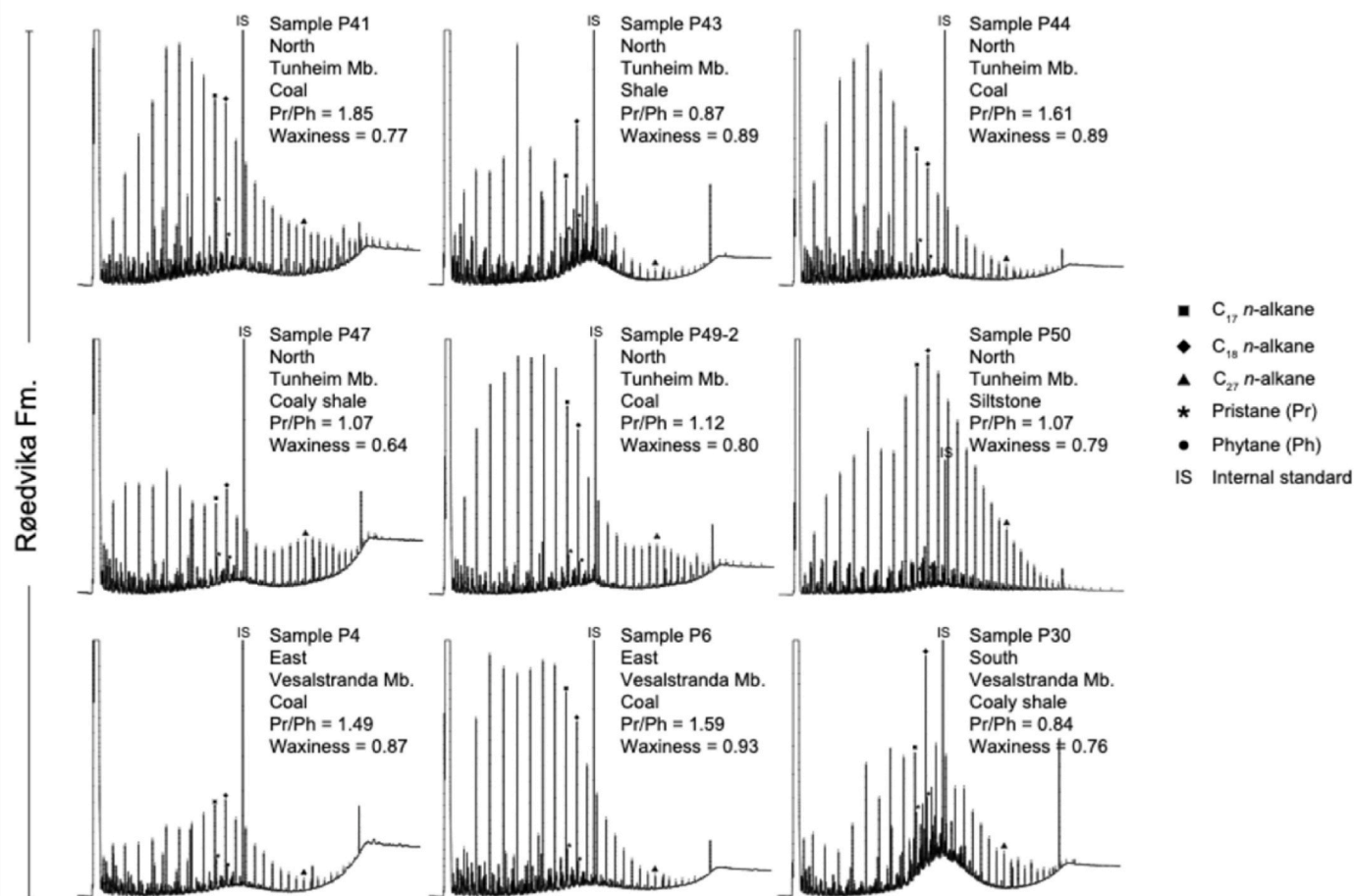


Fig. 8. GC-FID chromatograms of the saturate fraction of the extracts. Pr/Ph = Pristane/Phytane, Waxiness =  $n\text{-C}_{17}/(n\text{-C}_{17} + n\text{-C}_{27})$ .

Rm corresponds to deep burial of more than 4 km with an estimated geothermal gradient between 31 and 41 °C/km (Ritter et al., 1996; Suggate, 1998).

Several different biomarker ratios are commonly used to assess the maturity of source rocks. Each biomarker ratio performs reliably within a certain thermal maturity window. The higher the thermal maturity of the studied interval, the less reliable biomarkers become as they experience thermal cracking and eventually reach an equilibrium (e.g. Farimond et al., 1998; Aderoju and Bend, 2017). Furthermore, evidence suggests that biomarkers are influenced by paleo-depositional and palaeoecological factors, opening for the possibility that changes in biomarker ratios that are not related to thermal maturity (Aderoju and Bend, 2017). The unimodal distribution on n-alkanes points towards an elevated maturity. This is obvious by the poor signal-to-noise ratio, which significantly increase the uncertainties in derived ratios (Fig. 8). We therefore conclude, that for our dataset, biomarkers are not suitable to determine thermal maturity.

## 5.2. Source facies

The HI, which typically is used to assess kerogen quality and source facies, decreases with increasing maturity as the kerogen is subjected to thermal cracking (Bordenave et al., 1993). The present-day HI values of <200 mg HC/g TOC suggest in general gas potential for the Røedvika Formation coals (Fig. 12E). By considering the  $T_{\text{max}}$ -HI lines from Sykes and Snowdon (2002) (Fig. 6D) and by extrapolating the HI values to initial values, certain coals of the Vesalstranda and Tunheim Members could have had an initial HI > 300 mg HC/g TOC. These values correspond to a mixed kerogen Type III/II and may suggest some oil potential

(Peters and Cassa, 1994). This is intriguing, as the organic petrography indicates vitrinite as the dominant maceral group for all the coals and coaly shales (Table 2). However, two of the coal samples are conspicuously found to contain 100% collinite (Table 2), albeit a hint of cell structures may indicate the presence of telinite. The fluorescence within these samples may be related to H-rich desmocolinite macerals (Peters and Cassa, 1994), which could be attributed to dispersed sub-microscopic liptinite and/or diffusion of H-rich compounds migrated from nearby liptinite and/or amorphous organic matter within the coal seam (Tyson, 1995). Anoxic depositional conditions may lead to preferential preservation of organic matter at high maturities (Skarstein et al., 2022). The identified vitrinite may thus host notable amounts of H-rich compounds that have a kerogen Type II composition. As a result, the current HI values and the maceral composition suggest that the coals had a mixed kerogen Type III/II assemblage prior to maturation.

Another explanation of initial HI values corresponding to a mixed kerogen Type III/II assemblage is the potential occurrence of finely distributed algal OM within these coals, which is difficult or virtually impossible to detect using standard organic petrography (van Koeverden et al., 2011). Indeed, the low OI values (Fig. 6C), the Pr/n-C<sub>17</sub> vs. Ph/n-C<sub>18</sub> diagram (Fig. 9A) and the low Pr/Ph ratios of the coals may suggest that the EOM was generated from a mixed terrestrial/aquatic kerogen Type III/II assemblage (Fig. 9A–C, Shanmugam, 1985). In a case study of the lower Carboniferous Nordkapp Formation in northern Bjørnøya, van Koeverden et al. (2011) analysed a single coal sample which yielded an initial mixed kerogen Type II/III assemblage. Their study considered the presence of abundant tricyclic terpanes to represent algal OM in the coals, as tricyclic terpanes are common to samples rich in algal OM such as the unicellular algae *Tasmanites* (Aquino Neto

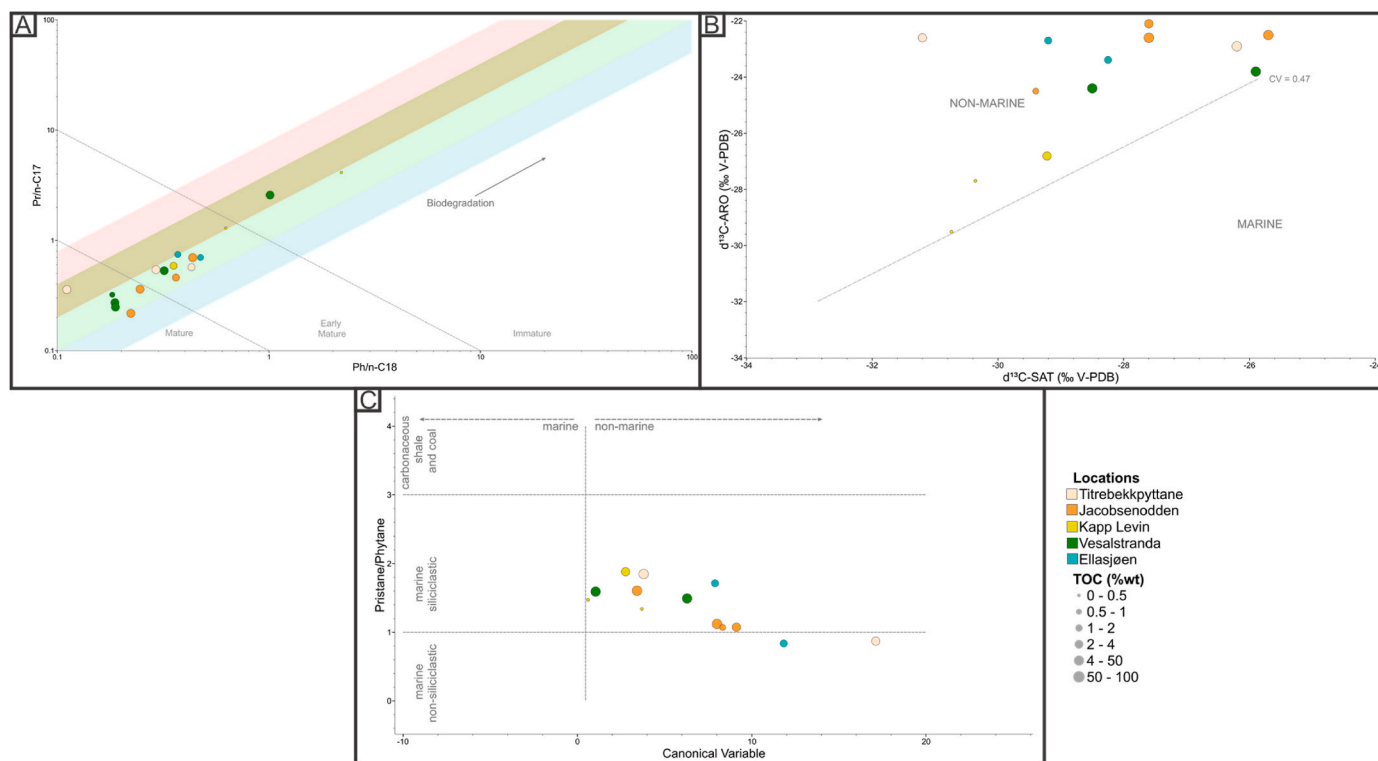


**Fig. 9.** (A) Scatter plot of Pr/n-C<sub>17</sub> vs. Ph/n-C<sub>18</sub>. The inferred process and elements adapted from Shanmugam (1985). (B) Scatter plot of  $\delta^{13}\text{C}_{\text{Aro}}$  vs.  $\delta^{13}\text{C}_{\text{Sat}}$ . The dashed line (CV = 0.47) separate the nonmarine and marine fields respectively (adapted from Sofer, 1984). (C) Scatter plot of the canonical variable (CV =  $-2.53 * \delta^{13}\text{C}_{\text{Sat}} + 2.22 * \delta^{13}\text{C}_{\text{Aro}} - 11.65$ ) vs. Pr/Ph. CV < 0.47 indicate marine OM-derived bitumen, while CV > 0.47 indicate nonmarine OM-derived bitumen as marked by the dashed vertical line (Sofer, 1984).

et al., 1992).

However, tricyclic terpanes are expelled to a proportionally larger extent than 30 $\alpha\beta$  hopane with increasing maturity, which may explain the high tricyclics/30 $\alpha\beta$  ratios in our samples (Peters and Moldowan, 1993). Furthermore, tricyclic terpanes may also be sourced by bacterial lipids and not necessarily from algae (Peters et al., 2005b). Ahmed et al. (2006) report abundant C<sub>19</sub> and C<sub>20</sub> tricyclic terpanes, C<sub>24</sub> tetracyclic terpane, but absent or low abundances of the extended tricyclic terpanes in late oil-overmature, vitrinite and inertinite-dominated (humic) Permian coals of the southern Sydney Basin, Australia. Our results thus appear to resemble that of Ahmed et al. (2006). Thus, while the identified tricyclic terpanes are commonly identified in oils or extracts from lacustrine and marine source rocks (Philp et al., 1989; Kruge et al., 1990; De Grande et al., 1993), their presence may not necessarily indicate algal OM within the coals of the Røedvika Formation. In fact, the lack of alginite macerals in the humic coals investigated in this study, rather suggest that lacustrine depositional conditions are unlikely for these coals (Table 2). Nevertheless, Gjelberg (1981) interpreted a lacustrine depositional environment for the thick siltstone unit in the lower part of the Kapp Levin Member at the Kapp Levin locality (Sample P52, P53 and P54 in this study). However, the siltstone unit, which is very different from the coals and occur at another stratigraphic level, cannot be used as evidence for a lacustrine environment for the coals. Furthermore, Devonian aged lacustrine deposits in the Orcadian Basin, Scotland, UK, exhibit the b-carotene marker in the saturate fraction GC-fingerprints (Peters et al., 1989). Interestingly, this marker was not identified in any of our samples (Fig. 8) and is also missing in contemporaneous lacustrine shales in northeast Greenland (Christiansen et al., 1990, 1992). Furthermore, no indicators for a lacustrine depositional setting have been described in the visual maceral observations.

Using the ternary plot of sterane biomarkers after Huang and Meinschein (1979) a transitional depositional environment between estuarine and terrestrial is indicated (Fig. 14). However, due to the high

maturity and the subsequent cracking of biomarkers the low biomarker intensities imply an uncertainty to the interpretation of biomarkers. Michelsen and Khorasani (1991) classified the coals of the Tunheim Member as humic given their dominance of vitrinite and inertinite (but consisting of up to 5 % of meta-liptines, i.e., vitrinite-resembling, matured sporinite). The relatively low Pr/Ph ratios of the coals could thus indicate reducing conditions and increased preservation of any H-rich liptinitic OM during deposition of these coals, perhaps facilitating a mixed kerogen Type III/II signature and low OI values. Radke et al. (2002) show that the Pr/Ph ratios of coals decrease with increasing maturity, from 10 in a coal sample with vitrinite reflectance of 0.9% Ro, to 1 in a coal sample with vitrinite reflectance of 1.7 %Ro. Thus, using Pr/Ph and the associated Pr/n-C<sub>17</sub> and Ph/n-C<sub>18</sub> ratios as indicators for source facies of the studied coals is uncertain.

This is also seen in Fig. 9A as Pr/n-C<sub>17</sub> and Ph/n-C<sub>18</sub> ratios suggest deposition in a mixed-transitional depositional environment (Shanmugam, 1985). However, based on the above discussion, a peat forming terrestrial environment would be expected for the coal samples of the Røedvika Formation. The elevated Pr/n-C<sub>17</sub> and Ph/n-C<sub>18</sub> ratios, however, can be a result of elevated maturities and/or aerobic biodegradation, where microbes prefer n-alkanes before the isoprenoids (Peters et al., 2005a). Again, Pr/n-C<sub>17</sub> and Ph/n-C<sub>18</sub> ratios are considered uncertain for the interpretation of the depositional environment.

The  $\delta^{13}\text{C}_{\text{Sat}}$  vs.  $\delta^{13}\text{C}_{\text{Aro}}$  plot (Fig. 9B) and the canonical variable (Fig. 9C) on the contrary shows that all samples plot in the non-marine field as defined by Sofer (1984). Though, our samples show quite some  $\delta^{13}\text{C}_{\text{Sat}}$  variability, ranging from  $-25.7$  ‰ in sample P44 to  $-31.2$  ‰ in sample P4. Both samples are from the Tunheim Member at the Jacobsenodden and Titrebekkyttane localities, respectively, and may reflect the diversity of the source organic matter in a delta-/floodplain depositional environment (APT report, supplementary material). In general, the high TOC coal samples show the most positive isotope values and vice versa for the shales/coal shales with less TOC and more negative

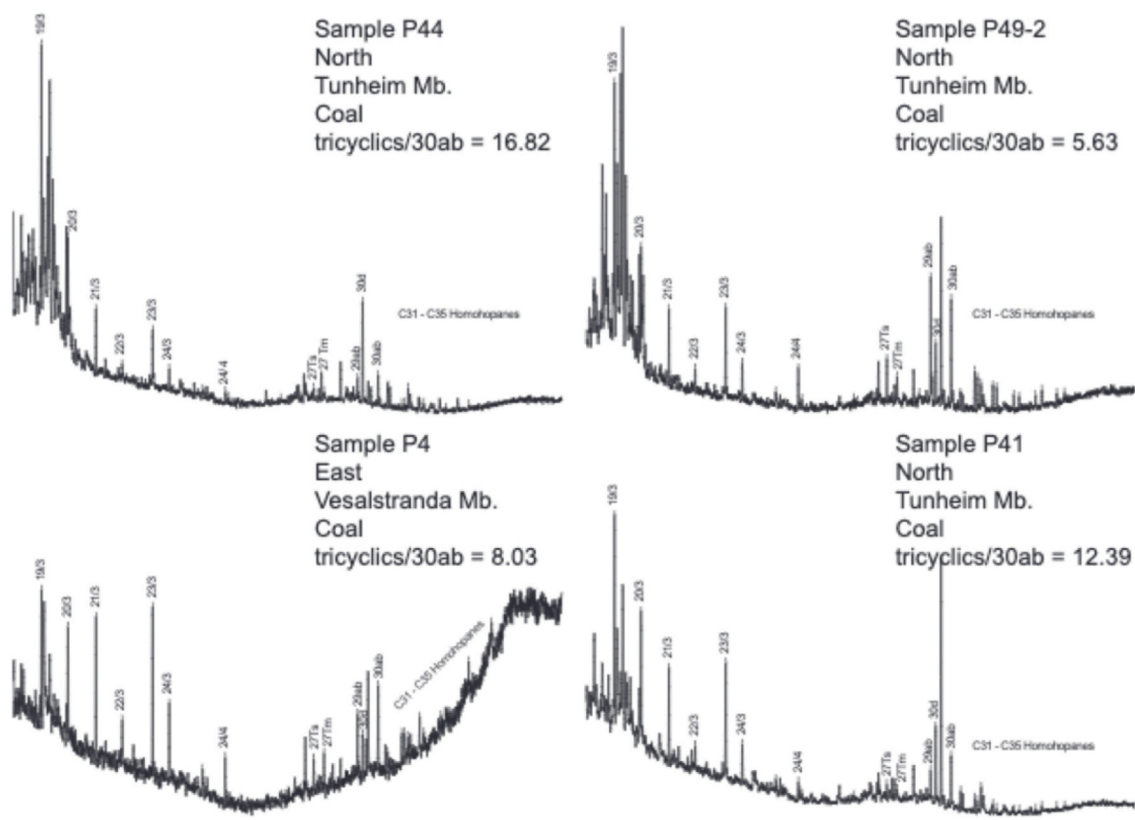


**Fig. 10.** m/z 191 fragmentograms of the saturate fraction of selected extracts. 19/3 to 24/3 = C<sub>19</sub> to C<sub>24</sub> tricyclic terpene. 24/4 = C<sub>24</sub> tetracyclic terpene. 27Ts = 18 $\alpha$ (H)-22,29,30-trisnorneohopane. 27 Tm = 17 $\alpha$ (H)-22,29,30-trisnorhopane. 29 $\alpha\beta$  = 17 $\alpha$ (H), 21 $\beta$ (H)-30-norhopane. 30d = 15 $\alpha$ -methyl-17 $\alpha$ (H)-27-norhopane (diahopane). 30 $\alpha\beta$  = 17 $\alpha$ (H), 21 $\beta$ (H)-hopane. Tricyclics/30 $\alpha\beta$  = sum of C<sub>19</sub>–C<sub>24</sub> tricyclic terpanes/30 $\alpha\beta$ .

isotope values. The isotopic signatures of our coal samples are in line with carbon isotope values reported by Peters-Kottig et al. (2006) for late Palaeozoic terrestrial organic matter (TOM). These authors also find a large spread in  $\delta^{13}\text{C}$ -TOM from approximate  $-22\text{‰}$  to  $-30\text{‰}$  in the Late Devonian and correlate it to changing atmospheric pCO<sub>2</sub>. Plants reflect the composition of atmospheric CO<sub>2</sub> as they incorporate it into their structure. Several factors can lead to a change in the composition of atmospheric CO<sub>2</sub>. Peters-Kottig et al. (2006) explain this Late Devonian pCO<sub>2</sub> variability with the development of early land plants and carbon burial leading to permanent storage of carbon and thereby altering the pCO<sub>2</sub> in the atmosphere. Another process they propose is the variability in  $\delta^{13}\text{C}_{\text{org}}$  in early land plant organic matter. In addition, Maynard (1981) reports organic carbon  $\delta^{13}\text{C}$  values of around  $-25\text{‰}$  in Devonian non-marine shale of the Appalachian Basin, intermediate values in prodelta environments, and values around  $-30\text{‰}$  in distal, basin settings. A negative isotope shift is also reported in transgressive marine black shale, deposited during the Famennian Hangenberg crisis (Pisarzowska et al., 2020). The negative isotope shift thus correlates with increased TOC values, suggesting a more anoxic depositional environment. Whether or not the observed isotope shift in our data relates to variations in organic matter input and/or significant spatio-temporal changes in the depositional environment, such as a transition from terrestrially dominated delta-/floodplain environments to marine or lacustrine deposition cannot be resolved, as our samples do not reveal biomarker data which would support one or the other theory.

### 5.2.1. Late Devonian climate and rift tectonics

Relatively few Devonian coals are known worldwide. Only by the Middle to Late Devonian, the rapid development and expansion of terrestrial vegetation enabled the accumulation of organic rich material which eventually could lithify into coal upon burial (Stein et al., 2007;

Davies and Gibling, 2010). Examples of Devonian coals are known from China (e.g. Dexin, 1989), Russia (e.g. Volkova, 1994), Canada (e.g. Goodarzi and Goodbody, 1990), and the USA (e.g. Cross and Phillips, 1990). In addition, coals are known from the Tordalen Formation (late Givetian to Frasnian) of the Middle to Upper Devonian Mimerdalen Subgroup on Spitsbergen (Vogt, 1941; Piepjohn and Dallmann, 2014; Blumenberg et al., 2018). Common for many of the above coals, is that they have been interpreted to have formed in terrestrial wetlands in paleo-equatorial settings, during a time of rapid plant colonization. This makes the Late Devonian-aged coals of Bjørnøya a rare deposit, which offers a window into the early formation of coals in fluvial/alluvial systems.

While the coals and coaly shale samples of the Vesalstranda Member show slightly higher HI and lower OI values compared to those of the Tunheim Member, it is evident that these coals largely exhibit the same organic facies (please refer to Table S1 in supplementary material). Hence, the depositional environment, which resulted in the accumulation of coals, appears to be rather similar for both units, with meandering fluvial channels transecting predominantly wet, yet vegetated floodplains. A conceptual and generalized depositional model of the Røedvika Formation coals, based on our logged sections and the geochemical signature of the deposits, is shown in Fig. 15. Thus, our proposed model is in line with the previous sedimentological investigations of the Røedvika Formation (Gjelberg, 1978, 1981; Worsley et al., 2001; Mørk et al., 2014).

Bjørnøya held a paleo-equatorial position during the Late Devonian and tropical conditions prevailed, resulting in a humid and warm climate that promoted the development of vegetated wetlands (Marshall et al., 2019; Lopes et al., 2021). Palynostratigraphic investigations indicate that the vegetation hosted lycopod *Cyclostigma kiltorkense* and progymnosperm *Archaeopteris*, the former considered the dominant

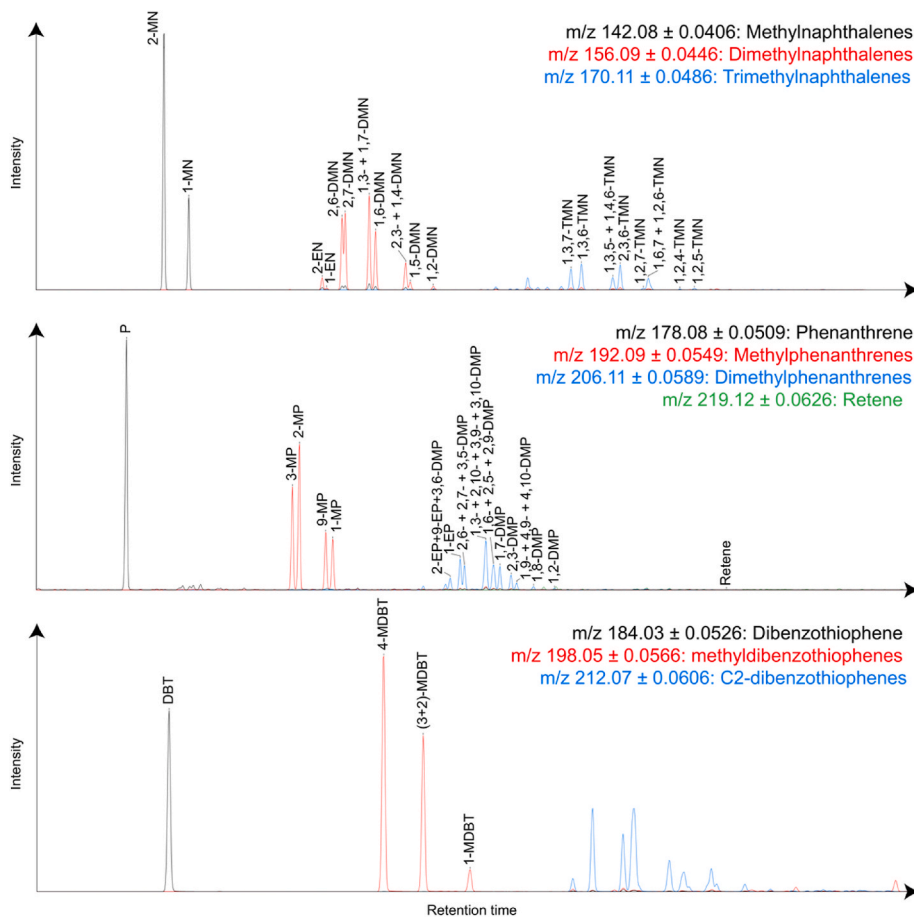


Fig. 11. Aromatic compounds of coal sample P4.

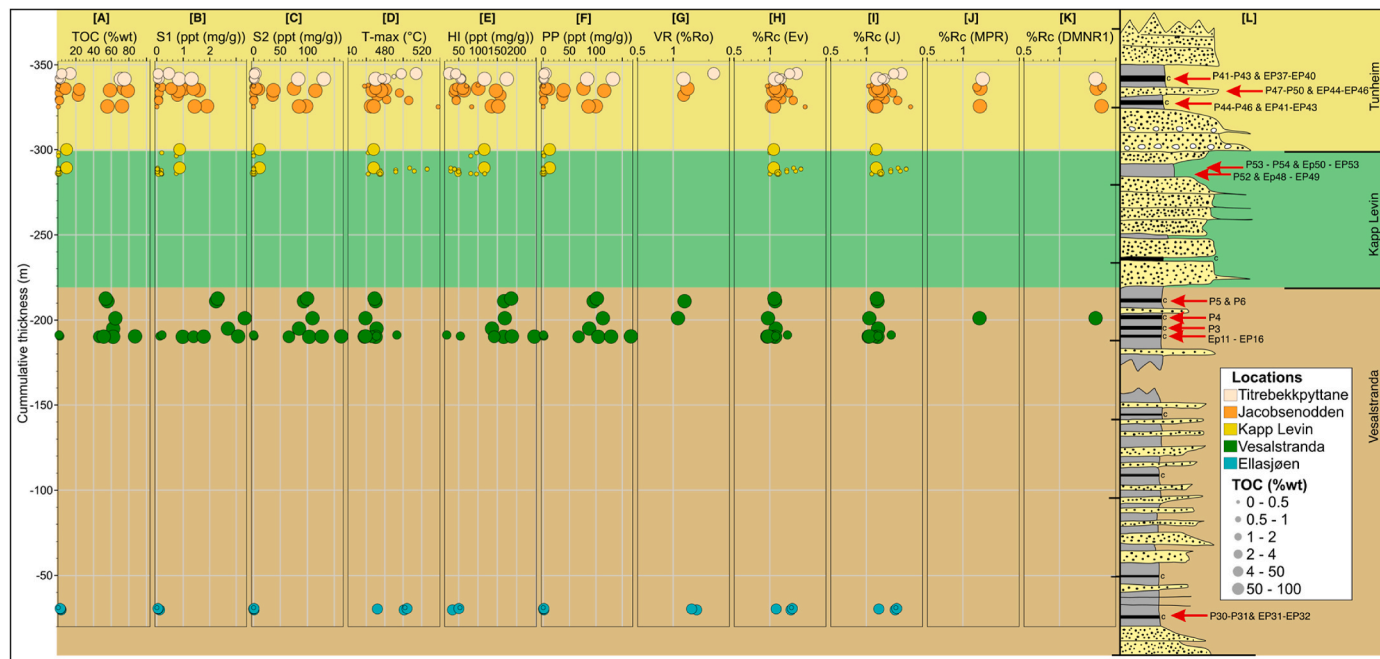


Fig. 12. Multi-depth plot of the Røedvika Formation Samples. (A) Total organic carbon (TOC) (B) measured S1 (C) measured S2 (D) T<sub>max</sub> (E) calculated Hydrogen Index (HI) (F) calculated Petroleum Potential (Hunt, 1996) (G) measured vitrinite reflectance (VR) (H) calculated vitrinite reflectance from T<sub>max</sub> after Evenick (2021) (I) calculated vitrinite reflectance from T<sub>max</sub> after Jarvie (2018) (J) calculated vitrinite reflectance from MPI-1 after Radke and Welte (1983) (K) calculated vitrinite reflectance from DMNR1 after Alexander et al. (1984) (L) composite stratigraphic Log after Gjelberg and Steel (1981), with members indicated to the right.

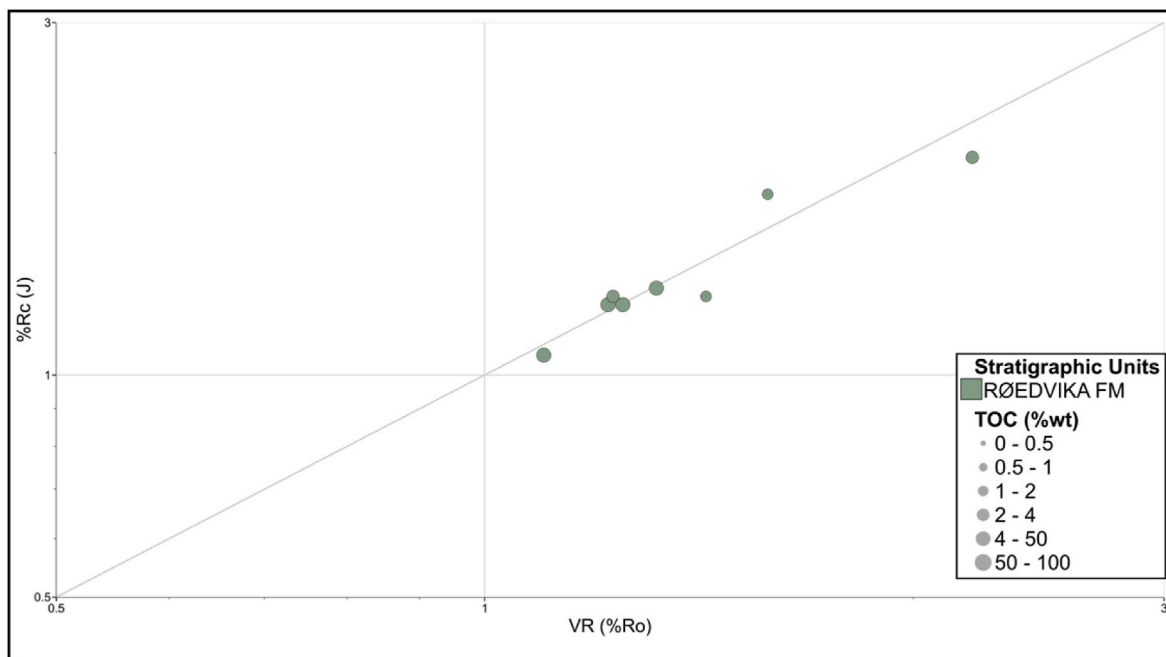


Fig. 13. Calculated vitrinite reflectance from  $T_{max}$  values after Jarvie (2018).

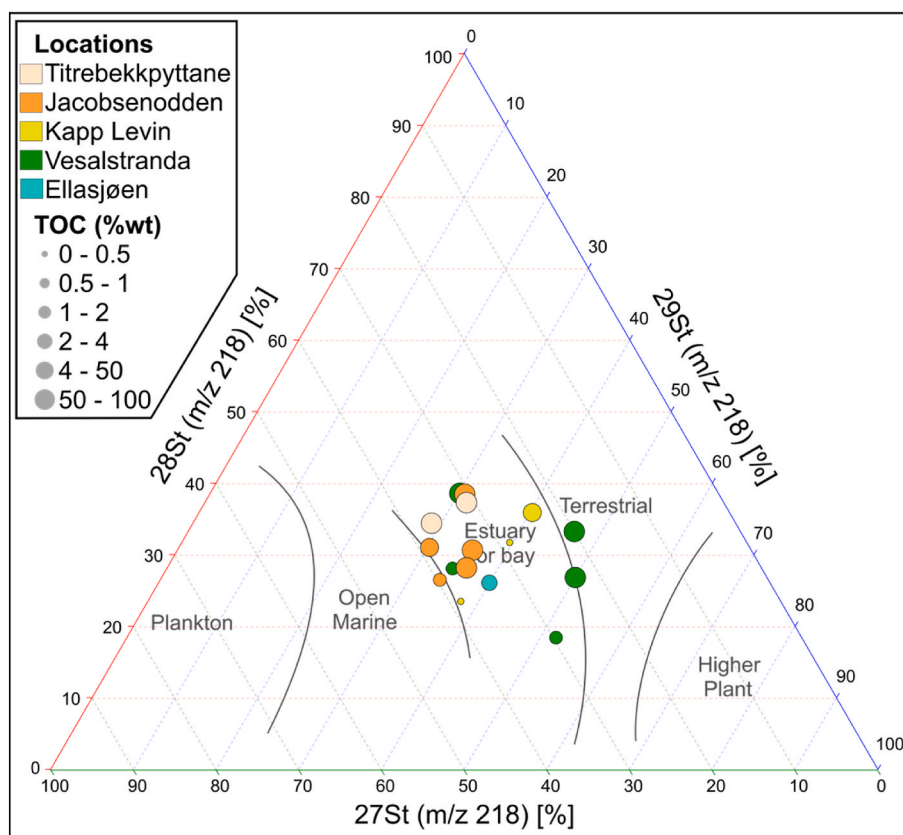


Fig. 14. Ternary plot of sterane biomarkers 27St, 28St and 29St after Huang and Meinschein (1979). Circle size indicates TOC while the colour coding refers to the sampling location.

contributor to the Vesalstranda Member coals (Marshall et al., 2019; Lopes et al., 2021). *Cyclostigma kiltorkense* appears to be less common during deposition of the overlying Tunheim Member coals (Lopes et al., 2021). Former investigations of Devonian paleo-equatorial humic coals in Nunavut, Arctic Canada, suggest that lycophytes were better adapted to

a water-saturated and anaerobic peat environment as their shallow roots could better handle a shallow anaerobic level, while *Archaeopteris* was most likely deeper-rooted and less adapted to such conditions (Marshall et al., 2019). Speculatively, the slightly larger HI and lower OI of the Vesalstranda Member coals relative to the Tunheim Member coals could

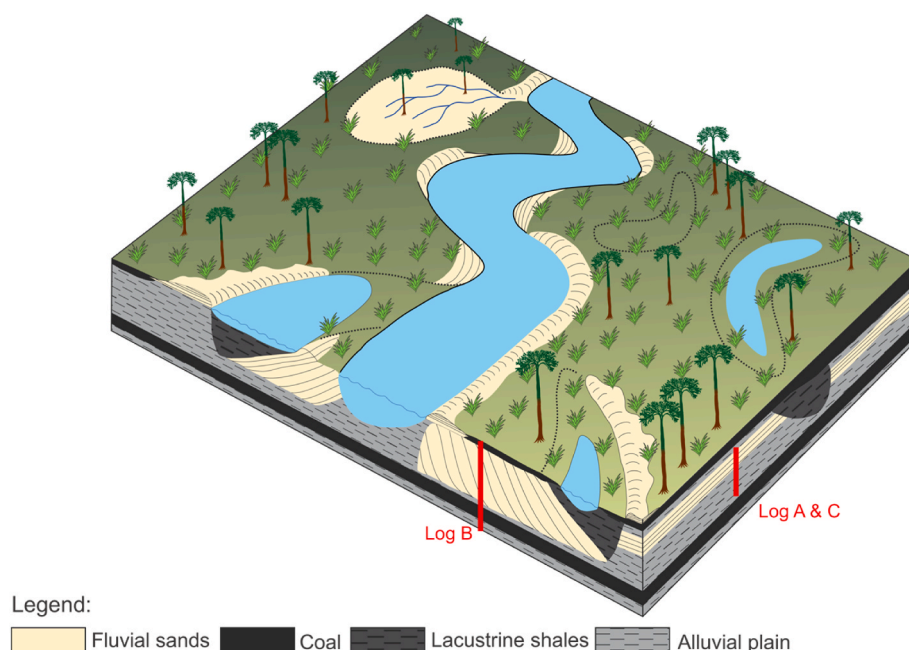


Fig. 15. Conceptual depositional model for the Vesalstranda and Tunheim Members of the Upper Devonian Røedvika Formation. Red columns indicate the relative positions of log locations A – C of Fig. 5. The model is partly based on McCabe (1985), as well as our own sedimentological and geochemical interpretations.

be attributed to a higher anaerobic layer, resulting in increased preservation of H-rich OM. The importance of changing terrestrial OM input on the resulting HI and OI is unknown.

Post Caledonian extensional tectonics and the establishment of major fault zones along the western margin of the Stappen High and Bjørnøya during the Late Devonian to earliest Carboniferous, seemingly created subsidence-induced lowlands which offered accommodation space (Fig. 3B–F,G,H,I) for the humid terrestrial clastic deposits to accumulate, concomitantly resulting in good preservation potential (Gjelberg, 1981, 1987; Gjelberg and Steel, 1983). On Bjørnøya the Upper Devonian was deposited east of the inferred Bjørnøya Fault, a major WSW trending, basin-bounding fault (Gjelberg, 1981; Gjelberg and Steel, 1983; Worsley et al., 2001). The thickest part of the Røedvika Formation is recorded on the north-eastern coastline of Bjørnøya where it reaches a thickness of 360 m. On the southwestern shoreline of Bjørnøya the Røedvika Formation thins to 100 m (Mørk et al., 2014). The alluvial strata of the Røedvika Formation have thus been strongly influenced by the activity of the inferred fault. Renewed subsidence led to the sudden creation of accommodation space, changing the depositional environments from floodplains and meandering streams to braided streams (Gjelberg, 1981; Gjelberg and Steel, 1983; Worsley et al., 2001; Mørk et al., 2014). The extensional tectonics and subsidence that created the basin may represent an early phase of the North Atlantic Rift System which, at a supra-regional scale, is associated with increased fault activity in the early Carboniferous (Rotevatn et al., 2018), or it may record a late phase of extension associated with the post Caledonian orogenic collapse (Gudlaugsson et al., 1998). Irrespective of the basin forming process, similar contemporaneous and lateral equivalent basins to the one on Bjørnøya have also been suggested to have occurred on the Loppa High further to the south on the Barents Shelf (Faleide et al., 1984; Gudlaugsson et al., 1998; Blaich et al., 2017). The timing of basin development on the Stappen High, where Bjørnøya is located, and the Loppa High, as well as the prevailing climatic conditions of the region during the Late Devonian, suggests that all the similar-aged basins on the western Barents Shelf probably provided ideal physiographic conditions for the accumulation of humid terrestrial deposits. Consequently, these basins are expected to host coals and other organic-rich deposits with a comparable mixed kerogen Type III/II signature, which potentially may

present source rock units of regional to semi-regional importance.

### 5.3. Petroleum potential

Oil expulsion from coals is a debated subject but believed to be possible and may, at least, have contributed to some oil discoveries around the World. Especially for thin coals which are interbedded with other clastic sediments, oil expulsion appears to be of a certain relevance as the migration path to the surrounding clastics is shorter. Other possibilities for oil expulsion are the migration of oils along fractures and cleats within the coals and very hydrogen-rich coals that generate oil (Wilkins and George, 2002). As the coal seams on Bjørnøya are mostly around 20 cm thick, except for the main A-coal seam which has a thickness of around 1 m (occasionally thicker), we can therefore assume that oil expulsion is a possibility from these thin seams. Advances in coal geology have shown that not only liptinites (exinites) but also vitrinite macerals can generate oil (Wilkins and George, 2002). Nonetheless we must stress the high maturity of the samples and the resulting alteration of their geochemical properties. The maceral analysis performed on a group of sub-samples (Table 1, samples marked in the VR column) document the oil generation potential of the coals and demonstrate the presence of live hydrocarbons (Table 2). This, on the other hand, is not supported by the low oil saturation index and the low  $S_1$  values reported for the same samples. Furthermore, in a re-evaluation of these specific samples, the live-oil could not be seen anymore, and prolific gas bubbles were observed. Explanations for this might be the evaporation of the oil over time and more firmly bound gas escape with further exposure to blue light. Most of the analysed samples are composed predominantly of collinite or to a less degree telinite (Table 2), both types which are known to generate oil (Tyson, 1995; Wilkins and George, 2002). Isaksen et al. (1998) found that HI values below 500 mg HC/g TOC in coals show poor correlation to the oil generation potential. Oil generation is therefore still possible from the coals in our dataset despite the relatively low HI values (Fig. 6C). Furthermore, the extrapolation of HI values from obtained  $T_{max}$  values shows potentially higher original HI values prior to deep burial and severe maturation (Fig. 6D). Considering our data, we thus conclude that the maceral content and the extrapolated HI of the Upper Devonian Vesalstranda and Tunheim Members, indicate a

good potential for generating liquid hydrocarbons. Our results thus conform to previous studies of the Billefjorden Group in Svalbard and the Barents Shelf (e.g. Bjørøy et al., 1980, 1983; Michelsen and Khorasani, 1991; van Koeverden et al., 2010, 2011; Nicolaisen et al., 2018), confirming its regional generation potential, but also expanding the stratigraphic significance of these source rocks to also encompass Upper Devonian coal-bearing strata. The contemporaneous rift basin developments on the Stappen and Loppa Highs besides the Bjørnøya Trough provided accommodation space in a similar climatic and tectonic setting as we infer for the Late Devonian basin on Bjørnøya (Gudlaugsson et al., 1998; Blaich et al., 2017). Therefore, we can assume that several of these basins potentially host source rocks with a good potential for hydrocarbon generation. Previous studies of Late Devonian to early Carboniferous basins on Svalbard and the Barents Shelf reportedly record lower maturities than revealed by our study (van Koeverden et al., 2010; Lasabuda et al., 2021). Basins located further south on the Stappen High and on the neighbouring Loppa High, on the other hand, experienced a similar burial and exhumation history to that of the Bjørnøya Trough (Laberg et al., 2012; Lasabuda et al., 2021). The consequence of the high maturities recorded here, is that the Upper Devonian and equivalent strata may previously have been over-estimated when it comes to the petroleum generation potential. In turn we predict that the Upper Devonian and lower Carboniferous potential source rocks have a lower significance than previously assumed. Therefore, the overall estimates for oil and gas reserves on the Barents Shelf are potentially too high. Nonetheless hydrocarbons may have been generated prior to deep burial, migrated into other strata, and may thus still be preserved, possibly contributing to mixed-source petroleum accumulations.

## 6. Conclusion

In this study we have analysed the organic geochemistry and source rock potential of 58 Upper Devonian to middle Permian coal and organic rich mudstone samples from the upper Palaeozoic succession on Bjørnøya, located on the exposed crest of the Stappen High on the western margin of the Norwegian Barents Shelf. Our combined geochemical and sedimentological investigations indicate the following.

- Vitrinite reflectance as well as calculated vitrinite reflectance from  $T_{max}$  and aromatic compounds show that the upper Palaeozoic succession on Bjørnøya has been deeply buried and subsequently undergone significant rates of uplift and erosion.
- The sampled coals, coaly shales and shales have reached a late oil to post-oil maturity.
- The maturity indicators from vitrinite reflectance and aromatic compounds indicate that the analysed aromatic compounds are sourced from the sampled intervals themselves and have not migrated.
- The high maturity resulted in the cracking of biomarkers, hence, the calculated  $R_c$  are encumbered with large uncertainties.
- The investigated coals of the Vesalstranda and Tunheim Members of the Upper Devonian (Famennian) Røedvika Formation of the Billefjorden Group are vitrinite-dominated, humic and show primarily a present-day kerogen Type III composition.
- The applied source facies parameters derived from *n*-alkanes and steranes all suggest a mixed kerogen Type III/II, however there are no unequivocal visual or geochemical evidence of marine or non-marine algal organic matter content as suggested by previous studies.
- The  $\delta^{13}C$  of the saturate and aromatic fractions, strongly suggests a non-marine organic matter signature, which thus indicates that any liptinite within the coals was derived from non-aqueous, terrestrial organic matter, in line with the fluvial/alluvial depositional setting interpreted by ours and previous sedimentological investigations.
- The coals probably accumulated in a fault bound, subsidence-created extensional basin characterized by a humid climate and wetland-

dominated fluvial/alluvial depositional environment at paleo-equatorial latitudes.

- The petroleum potential is the greatest for the coals of the Vesalstranda and Tunheim Members of the Røedvika Formation. Observed collinite and telinite macerals in the samples indicate that these coals have a good potential of generating liquid hydrocarbons. Extrapolating the HI-Index prior to burial indicates a Kerogen Type III-II source for the coals.
- The hydrocarbon generation potential is poor or absent for the other sampled lithologies and stratigraphic intervals, including thin coals and organic-rich deposits spanning the upper Carboniferous to middle Permian, as suggested by their back calculated HI-Indices which lie within the Kerogen Type IV window.
- The high maturity of the samples have resulted in a strong alteration of some geochemical properties. Consequently, previous studies on the generation potential may have over-estimated the generation potential of the Upper Devonian coals of Bjørnøya and similar coal deposits of the Billefjorden Group elsewhere on the Barents Shelf.

## CRedit authorship contribution statement

**Julian Janocha:** Formal analysis, Investigation, Project administration, Software, Validation, Visualization, Writing – original draft, Writing – review & editing. **Fredrik Wesenlund:** Data curation, Formal analysis, Investigation, Software, Visualization, Writing – original draft, Writing – review & editing. **Olaf Thießen:** Data curation, Formal analysis, Investigation, Resources, Software, Validation, Visualization, Writing – original draft, Writing – review & editing. **Sten-Andreas Grundvåg:** Conceptualization, Investigation, Project administration, Supervision, Visualization, Writing – original draft, Writing – review & editing. **Jean-Baptiste Koehl:** Investigation. **Erik P. Johannessen:** Investigation.

## Declaration of competing interest

The authors declare that they have no known competing financial interests or personal relationships that could have appeared to influence the work reported in this paper.

## Data availability

Data will be made available on request.

## Acknowledgments

This research received funding from the Research Council of Norway (grant numbers 228107 and 295208). We also acknowledge Rick Harding and Applied Petroleum Technology for their valuable input and re-evaluation of maceral descriptions. Furthermore, we thank Equinor for providing additional data and for the approval of publication. Tormod Henningsen (Equinor/pensioner), Gunnar Knag (Equinor/pensioner), Tore Forthun (Equinor), Marco Brønner (NGU), and Jomar Gellein (NGU) are thanked for their excellent comradeship in the field.

## Appendix A. Supplementary data

Supplementary data to this article can be found online at <https://doi.org/10.1016/j.marpetgeo.2024.106768>.

## References

- Abdullah, W.H., Murchison, D., Jones, J.M., Telnaes, N., Gjelberg, J.G., 1988. Lower carboniferous coal deposition environments on Spitsbergen, Svalbard. *Org. Geochem.* 13, 953–964.
- Aderoju, T., Bend, S., 2017. A comparative assessment of biomarker-based thermal maturity parameters. In: AbuAli, M.A., Moretti, I., Nordgård Bolås, H.M. (Eds.),

- Petroleum Systems Analysis - Case Studies: AAPG Memoir 114, pp. 219–237. <https://doi.org/10.1306/13602031M1143706>.
- Ahmed, M., Volk, H., George, S.C., Faiz, M., 2006. Organic geochemical characteristics of late permian coals from the southern Sydney Basin, Australia. In: Hutton, A., Griffin, J. (Eds.), 36th Sydney Basin Symposium on “Advances in the Study of the Sydney Basin”, 27–29 November, 2006. University of Wollongong, NSW 2522, Australia, pp. 149–156.
- Alexander, R., Kagi, R., Sheppard, P., 1984. 1,8-Dimethylnaphthalene as an indicator of petroleum maturity. *Nature* 308, 442–443. <https://doi.org/10.1038/308442a0>.
- Alexander, R., Kagi, R.I., Rowland, S.J., Sheppard, P.N., Chirila, T.V., 1985. The effects of thermal maturity on distributions of dimethylnaphthalenes and trimethylnaphthalenes in some Ancient sediments and petroleum. *Geochem. Cosmochim. Acta* 49, 385–395. [https://doi.org/10.1016/0016-7037\(85\)90031-6](https://doi.org/10.1016/0016-7037(85)90031-6).
- Alexander, R., Kagi, R.I., Sheppard, P.N., 1983. Relative abundance of dimethylnaphthalene isomers in crude oils. *J. Chromatogr. A* 267, 367–372. [https://doi.org/10.1016/s0021-9673\(01\)90855-6](https://doi.org/10.1016/s0021-9673(01)90855-6).
- Alsgaard, P.C., 1993. Eastern Barents Sea late palaeozoic setting and potential source rocks. In: Vorren, T.O., Bergsager, E., Dahl-Stammes, Ø.A., Holter, E., Johansen, B., Lie, E., Lund, T.B. (Eds.), *Arctic Geology and Petroleum Potential*. Elsevier, Amsterdam, pp. 405–418. <https://doi.org/10.1016/b978-0-444-88943-0.50030-7>.
- Aquino Neto, F.R., Trigüis, J., Azevedo, D.A., Rodrigues, R., Simoneit, B.R.T., 1992. Organic geochemistry of geographically unrelated tasmanites. *Org. Geochem.* 18, 791–803. [https://doi.org/10.1016/0146-6380\(92\)90048-3](https://doi.org/10.1016/0146-6380(92)90048-3).
- Bjørøy, M., Mørk, A., Vigran, J.O., 1983. Organic geochemical studies of the devonian to triassic succession on Bjørnøya and the implications for the Barents shelf. In: Bjørøy, M. (Ed.), *Advances in Organic Geochemistry 1981*. Wiley, Chichester, pp. 49–59.
- Bjørøy, M., Mørk, A., Vigran, J.O., Worsley, D., 1980. Organic Geochemistry of the Palaeozoic Sequence of Bjørnøya (Bear Island), Report (IKU). Continental Shelf Institute, Trondheim, Norway, pp. 1–58.
- Blaich, O.A., Tsikalas, F., Faleide, J.I., 2017. New insights into the tectono-stratigraphic evolution of the southern stappan high and its transition to Bjørnøya basin, SW Barents Sea. *Mar. Petrol. Geol.* 85, 89–105. <https://doi.org/10.1016/j.marpetgeo.2017.04.015>.
- Blumenberg, M., Weniger, P., Kus, J., Scheeder, G., Piepjohn, K., Zindler, M., Reinhardt, L., 2018. Geochemistry of a middle Devonian channel coal (Munindalen) in comparison with Carboniferous coals from Svalbard. *Arktos* 4, 1–8. <https://doi.org/10.1016/B978-0-08-037236-5.50028-2>.
- Bordenave, M.L., Espitalié, J., Leplat, P., Oudin, J.L., Vandenbroucke, M., 1993. Screening techniques for source rock evaluation. In: Bordenave, M.L. (Ed.), *Applied Petroleum Geochemistry*. Editions Technip, Paris, pp. 217–278.
- Bugge, T., Mangerud, G., Elvebakk, G., Mørk, A., Nilsson, I., Fanavoll, S., Vigran, J.O., 1995. The upper palaeozoic succession on the Finnmark platform, Barents Sea. *Norw. J. Geol.* 75, 3–30.
- Christiansen, F.G., Dam, G., Piasecki, S., Stemmerik, L., 1992. A review of Upper Palaeozoic and Mesozoic source rocks from onshore East Greenland. In: Spencer, A. M. (Ed.), *Special Publication of the European Association Petroleum Geologists* 2, pp. 151–161.
- Christiansen, F.G., Olsen, H., Piasecki, S., Stemmerik, L., 1990. Organic geochemistry of upper palaeozoic lacustrine shales in the East Greenland basin. *Org. Geochem.* 16, 287–294. [https://doi.org/10.1016/0146-6380\(90\)90048-5](https://doi.org/10.1016/0146-6380(90)90048-5).
- Cornford, C., 1998. Source rocks and hydrocarbons of the North sea. In: Glennie, K.W. (Ed.), *Petroleum Geology of the North Sea*. Blackwell Science Ltd., Oxford, UK, pp. 376–462. <https://doi.org/10.1002/9781444313413.ch11>.
- Cross, A.T., Phillips, T.L., 1990. Coal-forming through time in north America. *Int. J. Coal Geol.* 16, 1–46. [https://doi.org/10.1016/0166-5162\(90\)90012-n](https://doi.org/10.1016/0166-5162(90)90012-n).
- Dallmann, W.K., 1999. Lithostratigraphic Lexicon of Svalbard. Norwegian Polar Institute.
- Dallmann, W.K., Blomeier, D., Elvevold, S., Mørk, A., Olaussen, S., Grundvåg, S.-A., Bond, D., Hormes, A., 2019. Chapter 6: historical geology. In: Dallmann, W.K. (Ed.), *Geoscience Atlas of Svalbard*, second ed. ed. Norwegian Polar Institute, Tromsø, Norway, pp. 89–132.
- Dallmann, W.K., Krasil'Shchikov, A.A., 1996. Geological Map of Svalbard. 1: 50 000, Sheet D20G. Bjørnøya, vol. 27. Norwegian Polar Institute.
- Davies, N.S., Gibling, M.R., 2010. Cambrian to Devonian evolution of alluvial systems: the sedimentological impact of the earliest land plants. *Earth Sci. Rev.* 98, 171–200. <https://doi.org/10.1016/j.earscirev.2009.11.002>.
- De Grande, S.M.B., Aquino Neto, F.R., Mello, M.R., 1993. Extended tricyclic terpanes in sediments and petroleum. *Org. Geochem.* 20, 1039–1047. [https://doi.org/10.1016/0146-6380\(93\)90112-o](https://doi.org/10.1016/0146-6380(93)90112-o).
- Dembicki, H., 2009. Three common source rock evaluation errors made by geologists during prospect or play appraisals. *AAPG (Am. Assoc. Pet. Geol.) Bull.* 93, 341–356. <https://doi.org/10.1306/10.1306/10230808076>.
- Dexin, H., 1989. The features of Devonian coal-bearing deposits in South China, the People's Republic of China. *Int. J. Coal Geol.* 12, 209–223. [https://doi.org/10.1016/0166-5162\(89\)90052-9](https://doi.org/10.1016/0166-5162(89)90052-9).
- di Primio, R., Horsfield, B., 2006. From petroleum-type organofacies to hydrocarbon phase prediction. *AAPG (Am. Assoc. Pet. Geol.) Bull.* 90, 1031–1058. <https://doi.org/10.1306/02140605129>.
- Evenick, J.C., 2021. Examining the relationship between Tmax and vitrinite reflectance: an empirical comparison between thermal maturity indicators. *J. Nat. Gas Sci. Eng.* 91 <https://doi.org/10.1016/j.jngse.2021.103946>.
- Faleide, J.I., Gudlaugsson, S.T., Jacquart, G., 1984. Evolution of the western Barents Sea. *Mar. Petrol. Geol.* 1, 123–150. [https://doi.org/10.1016/0264-8172\(84\)90082-5](https://doi.org/10.1016/0264-8172(84)90082-5).
- Faleide, J.I., Tsikalas, F., Breivik, A.J., Mjelde, R., Ritzmann, O., Engen, Ø., Wilson, J., Eldholm, O., 2008. Structure and evolution of the continental margin off Norway and the Barents Sea. *Episodes* 31, 82–91. <https://doi.org/10.18814/epiugs/2008/v31i1/012>.
- Farrimond, P., Taylor, A., Telnæs, N., 1998. Biomarker maturity parameters: the role of generation and thermal degradation. *Org. Geochem.* 29, 1181–1197. [https://doi.org/10.1016/s0146-6380\(98\)00079-5](https://doi.org/10.1016/s0146-6380(98)00079-5).
- Gac, S., Hansford, P.A., Faleide, J.I., 2018. Basin modelling of the SW Barents Sea. *Mar. Petrol. Geol.* 95, 167–187. <https://doi.org/10.1016/j.marpetgeo.2018.04.022>.
- Gjelberg, J.G., 1978. The upper devonian (Famennian)/Middle carboniferous (? Muscovian) strata on Bjørnøya (svalbard) - a study in alluvial and coastal marine sedimentology. *Sedimentology*. University of Bergen, Bergen.
- Gjelberg, J.G., 1981. Upper Devonian (Famennian)-Middle Carboniferous succession of Bjørnøya: a study of ancient alluvial and coastal marine sedimentation. *Nor. Polarinst. Skr.* 174.
- Gjelberg, J.G., 1987. Early carboniferous graben style and sedimentation response, svalbard. In: Miller, J., Adams, A.E., Wright, V.P. (Eds.), *European Dinanint Environments*. John Wiley & Sons Ltd., pp. 93–113.
- Gjelberg, J.G., Steel, R.J., 1981. An outline of Lower-Middle Carboniferous sedimentation on Svalbard: effects of tectonic, climatic and sea level changes in rift basin sequences. In: Kerr, J.W. (Ed.), *Geology of the North Atlantic Borderlands*. Canadian Society of Petroleum Geology, Calgary, pp. 543–563.
- Gjelberg, J.G., Steel, R.J., 1983. Middle Carboniferous marine transgression, Bjørnøya, Svalbard: facies sequences from an interplay of sea level changes and tectonics. *Geol. J.* 18, 1–19.
- Golonka, J., 2020. Late Devonian paleogeography in the framework of global plate tectonics. *Global Planet. Change* 186. <https://doi.org/10.1016/j.gloplacha.2020.103129>.
- Goodarzi, F., Goodbody, Q., 1990. Nature and depositional environment of Devonian coals from western Melville island, Arctic Canada. *Int. J. Coal Geol.* 14, 175–196. [https://doi.org/10.1016/0166-5162\(90\)90002-g](https://doi.org/10.1016/0166-5162(90)90002-g).
- Grogan, P., Østvedt-Ghazi, A.M., Larssen, G.B., Fotland, B., Nyberg, K., Dahlgren, S., Eidvin, T., 1999. Structural elements and petroleum geology of the Norwegian sector of the northern Barents Sea. *Geological Society, London, Petroleum Geology Conference Series* 5, 247–259. <https://doi.org/10.1144/0050247>.
- Grundvåg, S.-A., Strand, M.S., Paulsen, C., Simonsen, B.T., Rostad, J., Mørk, A., Mørk, M. B.E., 2023. The Hambergfjellet Formation on Bjørnøya – sedimentary response to early permian tectonics on the stappan high. *Norw. J. Geol.* <https://doi.org/10.17850/njg1031-2>.
- Gudlaugsson, S.T., Faleide, J.I., Johansen, S.E., Breivik, A.J., 1998. Late palaeozoic structural development of the south-western Barents Sea. *Mar. Petrol. Geol.* 15, 73–102. [https://doi.org/10.1016/s0264-8172\(97\)00048-2](https://doi.org/10.1016/s0264-8172(97)00048-2).
- Hagset, A., Grundvåg, S.A., Badics, B., Davies, R., Rotevatn, A., 2022. Tracing lower cretaceous organic-rich units across the SW Barents shelf. *Mar. Petrol. Geol.* 140 <https://doi.org/10.1016/j.marpetgeo.2022.105664>.
- Henriksen, E., Ryseth, A.E., Larssen, G.B., Heide, T., Rønning, K., Sollid, K., Stoupakova, A.V., 2011. Chapter 10 - tectonostratigraphy of the greater Barents Sea: implications for petroleum systems. In: Spencer, A.M., Embry, A.F., Gautier, D.L., Stoupakova, A.V., Sørensen, K. (Eds.), *Arctic Petroleum Geology*. Geological Society, London, Memoirs, pp. 163–195. <https://doi.org/10.1144/M35.10>.
- Horn, G., Orvin, A.K., 1928. Geology of Bear Island: with Special Reference to the Coal Deposits, and with an Account of the History of the Island, Skriften Om Svalbard Og Ishavet Nr, vol. 15. Oslo, Norway. <http://hdl.handle.net/11250/173572>.
- Huang, W.-Y., Meinschein, W.G., 1979. Sterols as ecological indicators. *Geochem. Cosmochim. Acta* 43, 739–745. [https://doi.org/10.1016/0016-7037\(79\)90257-6](https://doi.org/10.1016/0016-7037(79)90257-6).
- Hunt, J.M., 1996. *Petroleum Geochemistry and Geology*, second ed. W.H. Freeman, New York.
- Isaksen, G.H., Curry, D.J., Yeakel, J.D., Jenssen, A.I., 1998. Controls on the oil and gas potential of humic coals. *Org. Geochem.* 29, 23–44. [https://doi.org/10.1016/s0146-6380\(98\)00042-4](https://doi.org/10.1016/s0146-6380(98)00042-4).
- Jarvie, D., 2018. Correlation of Tmax and Measured Vitrinite Reflectance. *Johannessen, E.P., Steel, R.J., 1992. Mid-Carboniferous extension and rift-infill sequences in the Billefjorden Trough, svalbard. Norw. J. Geol.* 72, 35–48.
- Justwan, H., Dahl, B., Isaksen, G.H., 2006. Geochemical characterisation and genetic origin of oils and condensates in the South Viking Graben, Norway. *Mar. Petrol. Geol.* 23, 213–239. <https://doi.org/10.1016/j.marpetgeo.2005.07.003>.
- Kaiser, H., 1970. Die Oberdevon-Flora der Bäreninsel : 3.Mikroflora des höheren Oberdevons und des Unterkarbons. *Palaeontographica* 129, 71–124.
- Kruger, M.A., Hubert, J.F., Bensley, D.F., Crelling, J.C., Akes, R.J., Meriney, P.E., 1990. Organic geochemistry of a lower jurassic synrift lacustrine sequence, Hartford Basin, Connecticut, U.S.A. *Organic Geochemistry* 16, 689–701. [https://doi.org/10.1016/0146-6380\(90\)90110-1](https://doi.org/10.1016/0146-6380(90)90110-1).
- Kvalheim, O.M., Christy, A.A., Telnæs, N., Bjørseth, A., 1987. Maturity determination of organic matter in coals using the methylphenanthrene distribution. *Geochem. Cosmochim. Acta* 51, 1883–1888. [https://doi.org/10.1016/0016-7037\(87\)90179-7](https://doi.org/10.1016/0016-7037(87)90179-7).
- Laberg, J.S., Andreassen, K., Vorren, T.O., 2012. Late Cenozoic erosion of the high-latitude southwestern Barents Sea shelf revisited. *Geol. Soc. Am. Bull.* 124, 77–88. <https://doi.org/10.1130/b30340.1>.
- Larssen, G.B., Elvebakk, G., Henriksen, L.B., Kristensen, S.E., Nilsson, I., Samuelsberg, T. J., Svånå, T.A., Stemmerik, L., Worsley, D., 2002. Upper Palaeozoic lithostratigraphy of the Southern Norwegian Barents Sea. *Norwegian Petroleum Directorate Bulletin* 9, 76.
- Larssen, G.B., Elvebakk, G., Henriksen, L.B., Kristensen, S.E., Nilsson, I., Samuelsberg, T. J., Svånå, T.A., Stemmerik, L., Worsley, D., 2005. Upper Palaeozoic lithostratigraphy of the southern part of the Norwegian Barents Sea. *Nor. Geol. Unders. Bull.* 444, 3–45.
- Lasubada, A., Laberg, J.S., Knutsen, S.-M., Høgseth, G., 2018. Early to middle Cenozoic paleoenvironment and erosion estimates of the southwestern Barents Sea: Insights

- from a regional mass-balance approach. *Mar. Petrol. Geol.* 96, 501–521. <https://doi.org/10.1016/j.marpetgeo.2018.05.039>.
- Lasabuda, A.P.E., Johansen, N.S., Laberg, J.S., Faleide, J.I., Senger, K., Rydningen, T.A., Patton, H., Knutsen, S.-M., Hanssen, A., 2021. Cenozoic uplift and erosion of the Norwegian Barents Shelf – A review. *Earth Sci. Rev.* 217 <https://doi.org/10.1016/j.earscirev.2021.103609>.
- Lopes, G., Mangerud, G., Clayton, G., Vigran, J.O., 2021. Palynostratigraphic reassessment of the Late Devonian of Bjørnøya, Svalbard. *Rev. Palaeobot. Palynol.* 286 <https://doi.org/10.1016/j.revpaalbo.2020.104376>.
- Lutz, R., Klitzke, P., Weniger, P., Blumberg, M., Franke, D., Reinhardt, L., Ehrhardt, A., Berglar, K., 2021. Basin and petroleum systems modelling in the northern Norwegian Barents Sea. *Mar. Petrol. Geol.* 130 <https://doi.org/10.1016/j.marpetgeo.2021.105128>.
- Marshall, J.E.A., Tel'nova, O.P., Berry, C.M., 2019. Devonian and Early Carboniferous coals and the evolution of wetlands. *Vestnik of Institute of Geology of Komi Science Center of Ural Branch RAS* 10, 12–15. <https://doi.org/10.19110/2221-1381-2019-10-12-15>.
- Matapour, Z., Karlsen, D.A., Lerch, B., Backer-Owe, K., 2019. Petroleum occurrences in the carbonate lithologies of the Gohta and Alta discoveries in the Barents Sea, Arctic Norway. *Petrol. Geosci.* 25, 50–70. <https://doi.org/10.1144/petgeo2017-085>.
- Maynard, J.B., 1981. Carbon isotopes as indicators of dispersal patterns in Devonian-Mississippian shales of the Appalachian Basin. *Geology* 9. [https://doi.org/10.1130/0091-7613\(1981\)9<262:Ciaiod>2.0.Co;2](https://doi.org/10.1130/0091-7613(1981)9<262:Ciaiod>2.0.Co;2).
- McCabe, P.J., 1985. Depositional Environments of Coal and Coal-Bearing Strata. In: Rahmani, R.A., Flores, R.M. (Eds.), *Sedimentology of Coal and Coal-Bearing Sequences*, pp. 11–42. <https://doi.org/10.1002/9781444303797.ch2>.
- Michelsen, J.K., Khorasani, G.K., 1991. A regional study on coals from Svalbard: organic facies, maturity and thermal history. *Bull. Soc. Geol. Fr.* 385–397.
- Moi, R., 2008. Oil-prone Carboniferous coals (Tettegras Fm.) from the Finnmark Platform: Implications for an alternative and new Petroleum System based on oil generative coals of the Billefjord Gr. In: *The Barents Region*. Department of Geosciences. University of Oslo, Oslo, Norway.
- Mørk, A., Gjelberg, J.G., Worsley, D., 2014. Bjørnøya: an Upper Paleozoic-Triassic Window into the Barents Shelf. *Geological Society of Norway*.
- Nicolaisen, J.B., Elvebakk, G., Ahokas, J., Bojesen-Koefoed, J.A., Olausen, S., Rinna, J., Skeie, J.E., Stemmerik, L., 2018. Characterization of Upper Palaeozoic Organic-Rich Units in Svalbard: Implications for the Petroleum Systems of the Norwegian Barents Shelf. *J. Petrol. Geol.* 42, 59–78. <https://doi.org/10.1111/jpg.12724>.
- Norwegian Petroleum Directorate, 2022. *Geostandard. Equinor*.
- Norwegian Petroleum Directorate, 2017. *Geological Assessment of Petroleum Resources in Eastern Parts of the Barents Sea North*. Norwegian Petroleum Directorate.
- Norwegian Polar Institute, 2016. *Geological Map of Svalbard (1:250000) [Data Set]*. Norwegian Polar Institute. <https://doi.org/10.21334/npolar.2016.616f7504>.
- Nøttvedt, A., Cecchi, M., Gjelberg, J.G., Kristensen, S.E., Lønøy, A., Rasmussen, A., Rasmussen, E., Skott, P.H., van Veen, P.M., 1993. Svalbard-Barents Sea correlation: a short review. In: Vorren, T.O., Bergsager, E., Dahl-Stammes, Ø.A., Holter, E., Johansen, B., Lie, E., Lund, T.B. (Eds.), *Arctic Geology and Petroleum Potential*. Elsevier, Amsterdam, pp. 363–375. <https://doi.org/10.1016/b978-0-444-88943-0.50027-7>.
- Ohm, S.E., Karlsen, D.A., Austin, T.J.F., 2008. Geochemically driven exploration models in uplifted areas: Examples from the Norwegian Barents Sea. *AAPG (Am. Assoc. Pet. Geol.) Bull.* 92, 1191–1223. <https://doi.org/10.1306/06180808028>.
- Olausen, S., Grundvåg, S.-A., Senger, K., Anell, I., Betlem, P., Birchall, T., Braathen, A., Dallmann, W., Jochmann, M., Johannessen, E.P., Lord, G., Mørk, A., Osmundsen, P. T., Smyrak-Sikora, A., Stemmerik, L., 2023. Svalbard Composite Tectono-Sedimentary Element, Barents Sea. *Geological Society, London, Memoirs* 57. <https://doi.org/10.1144/m57-2021-36>.
- Peters, K.E., Cassa, M.R., 1994. *Applied Source Rock Geochemistry*. In: Magoon, L.B., Dow, W.G. (Eds.), *The Petroleum System - from Source to Trap: AAPG Memoir 60*. The American Association of Petroleum Geologists, Tulsa, Oklahoma, U.S.A., pp. 93–120.
- Peters, K.E., Moldowan, J.M., 1993. *The Biomarker Guide: Interpreting Molecular Fossils in Petroleum and Ancient Sediments*. Prentice-Hall, Englewood Cliffs, N. J.
- Peters, K.E., Moldowan, J.M., Driscoll, A.R., Demaison, G.J., 1989. Origin of Beatrice Oil by Co-Sourcing from Devonian and Middle Jurassic Source Rocks, Inner Moray Firth, United Kingdom. *AAPG (Am. Assoc. Pet. Geol.) Bull.* 73, 454–471. <https://doi.org/10.1306/44b49fce-170a-11d7-8645000102c1865d>.
- Peters, K.E., Walters, C.C., Moldowan, J.M., 2005a. *The Biomarker Guide: I Biomarkers and Isotopes in the Environment and Human History*, 2 ed. Cambridge University Press, Cambridge.
- Peters, K.E., Walters, C.C., Moldowan, J.M., 2005b. *The Biomarker Guide: II Biomarkers and Isotopes in Petroleum Systems and Earth History*, 2 ed. Cambridge University Press, Cambridge.
- Peters-Kottig, W., Strauss, H., Kerp, H., 2006. The land plant  $\delta^{13}C$  record and plant evolution in the Late Palaeozoic. *Palaeogeogr. Palaeoclimatol. Palaeoecol.* 240, 237–252. <https://doi.org/10.1016/j.palaeo.2006.03.051>.
- Petrov, O., Sobolev, N.N., Koren, T.N., Vasiliev, V.E., Petrov, E.O., Larssen, G.B., Smelror, M., 2008. Palaeozoic and Early Mesozoic evolution of the East Barents and Kara Seas sedimentary basins. *Norw. J. Geol.* 88, 227–234.
- Philp, R.P., Jingui, L., Lewis, C.A., 1989. An organic geochemical investigation of crude oils from Shanganning, Jiangnan, Chaidamir and Zhungeer Basins, People's Republic of China. *Org. Geochem.* 14, 447–460. [https://doi.org/10.1016/0146-6380\(89\)90010-7](https://doi.org/10.1016/0146-6380(89)90010-7).
- Piepijohann, K., Dallmann, W.K., 2014. Stratigraphy of the uppermost Old Red Sandstone of Svalbard (Mimerdalen Subgroup). *Polar Res.* 33 <https://doi.org/10.3402/polar.v33.19998>.
- Pisarszowska, A., Rakociński, M., Marynowski, L., Szczerba, M., Thoby, M., Paszkowski, M., Perri, M.C., Spalletta, C., Schönlaub, H.-P., Kowalik, N., Gereke, M., 2020. Large environmental disturbances caused by magmatic activity during the Late Devonian Hangenberg Crisis. *Global Planet. Change* 190. <https://doi.org/10.1016/j.gloplacha.2020.103155>.
- Radke, M., 1988. Application of aromatic compounds as maturity indicators in source rocks and crude oils. *Mar. Petrol. Geol.* 5, 224–236. [https://doi.org/10.1016/0264-8172\(88\)90003-7](https://doi.org/10.1016/0264-8172(88)90003-7).
- Radke, M., Welte, D.H., 1983. The methylphenanthrene index (MPI). A maturity parameter based on aromatic hydrocarbons. In: Bjørøy, M., Albrecht, P., Corner, G. D., de Groot, K., Eglinton, G., Galimov, E., Leythaeuser, D., Pelet, R., Rullkötter, J., Speers, G. (Eds.), *Advances in Organic Geochemistry 1981*. John Wiley & Sons, Chichester, pp. 504–512.
- Radke, M., Welte, D.H., Willsch, H., 1982a. Geochemical study on a well in the Western Canada Basin: relation of the aromatic distribution pattern to maturity of organic matter. *Geochem. Cosmochim. Acta* 46, 1–10. [https://doi.org/10.1016/0016-7037\(82\)90285-x](https://doi.org/10.1016/0016-7037(82)90285-x).
- Radke, M., Willsch, H., Leythaeuser, D., Teichmüller, M., 1982b. Aromatic Components of Coal - Relation of Distribution Pattern to Rank. *Geochem. Cosmochim. Acta* 46, 1831–1848. [https://doi.org/10.1016/0016-7037\(82\)90122-3](https://doi.org/10.1016/0016-7037(82)90122-3).
- Radke, M., Willsch, H., Welte, D.H., 2002. Preparative hydrocarbon group type determination by automated medium pressure liquid chromatography. *Anal. Chem.* 74, 406–411. <https://doi.org/10.1021/ac50053a009>.
- Ritter, U., Duddy, I.R., Mork, A., Johansen, H., Arne, D.C., 1996. Temperature and uplift history of Bjørnøya (Bear Island), Barents Sea. *Petrol. Geosci.* 2, 133–144. <https://doi.org/10.1144/petgeo.2.2.133>.
- Rotevatn, A., Kristensen, T.B., Ksienzyk, A.K., Wemmer, K., Henstra, G.A., Midtkandal, I., Grundvåg, S.A., Andresen, A., 2018. Structural Inheritance and Rapid Rift-Length Establishment in a Multiphase Rift: The East Greenland Rift System and its Caledonian Orogenic Ancestry. *Tectonics* 37, 1858–1875. <https://doi.org/10.1029/2018tc005018>.
- Ryseth, A.E., Similox-Tohon, D., Thieben, O., 2021. Tromsø-Bjørnøya Composite Tectono-Sedimentary Element, Barents Sea. *Geological Society, London, Memoirs* 57. <https://doi.org/10.1144/m57-2018-19>.
- Senger, K., Brugmans, P., Grundvåg, S.-A., Jochmann, M., Nøttvedt, A., Olausen, S., Skotte, A., Smyrak-Sikora, A., 2019. Petroleum, coal and research drilling onshore Svalbard: a historical perspective. *Norw. J. Geol.* <https://doi.org/10.17850/njg99-3-1>.
- Shanmugam, G., 1985. Significance of Coniferous Rain Forests and Related Organic Matter in Generating Commercial Quantities of Oil, Gippsland Basin, Australia. *AAPG (Am. Assoc. Pet. Geol.) Bull.* 69, 1241–1254. <https://doi.org/10.1306/ad462bc3-16f7-11d7-8645000102c1865d>.
- Skarstein, G., Ohm, S., Cedeño, A., Escalona, A., 2022. Facies variations in the Upper Jurassic source rocks of the Norwegian North Sea: from micro- to macro scale. *Mar. Petrol. Geol.* 145 <https://doi.org/10.1016/j.marpetgeo.2022.105856>.
- Smelror, M., Olausen, S., Grundvåg, S.-A., Dallmann, W.K., Dumais, M.-A., 2024. Northern Svalbard Composite Tectono-Stratigraphic Element, Sedimentary successions of the Arctic Region and their hydrocarbon prospectivity. *Geological Society, London*. <https://doi.org/10.1144/M57-2023-2>.
- Smelror, M., Petrov, O., Larssen, G.B., Werner, S., 2009. *The Geological History of the Barents Sea*. Geological Survey of Norway, Trondheim, Norway.
- Smelror, M., Petrov, O.V., 2018. Geodynamics of the Arctic: From proterozoic orogens to present day seafloor spreading. *J. Geodyn.* 121, 185–204. <https://doi.org/10.1016/j.jog.2018.09.006>.
- Smyrak-Sikora, A., Johannessen, E.P., Olausen, S., Sandal, G., Braathen, A., 2018. Sedimentary architecture during Carboniferous rift initiation – the arid Billefjorden Trough, Svalbard. *J. Geol. Soc.* 176, 225–252. <https://doi.org/10.1144/jgs2018-100>.
- Sobolev, P., 2018. Source rock evaluation and petroleum system modeling of the South Barents and South Kara basins. *arXiv* 4, 1–9. <https://doi.org/10.1007/s41063-018-0039-x>.
- Sofer, Z., 1984. Stable Carbon Isotope Compositions of Crude Oils - Application to Source Depositional-Environments and Petroleum Alteration. *AAPG Bull.* 68, 31–49. <https://doi.org/10.1306/AD460963-16F7-11D7-8645000102C1865D>.
- Stein, W.E., Mannolini, F., Hernick, L.V., Landing, E., Berry, C.M., 2007. Giant cladoxylous trees resolve the enigma of the Earth's earliest forest stumps at Gilboa. *Nature* 446, 904–907. <https://doi.org/10.1038/nature05705>.
- Stemmerik, L., 1997. Permian (Artinskian-Kazanian) Cool-Water Carbonates in North Greenland, Svalbard and the Western Barents Sea. In: James, N.P., Clark, J.A.D. (Eds.), *Cool-Water Carbonates*. Society for Sedimentary Geology, Tulsa, Oklahoma, U.S.A., pp. 349–364. <https://doi.org/10.2110/pec.97.56.0349>.
- Stemmerik, L., Christiansen, F.G., Piasecki, S., Jordt, B., Marcussen, C., Nøhr-Hansen, H., 1993. Depositional history and petroleum geology of the Carboniferous to Cretaceous sediments in the northern part of East Greenland. In: Vorren, T.O., Bergsager, E., Dahl-Stammes, Ø.A., Holter, E., Johansen, B., Lie, E., Lund, T.B. (Eds.), *Arctic Geology and Petroleum Potential*. Elsevier, Amsterdam, pp. 67–87. <https://doi.org/10.1016/b978-0-444-88943-0.50009-5>.
- Stemmerik, L., Worsley, D., 2000. Upper Carboniferous cyclic shelf deposits, Kapp Kåre Formation, Bjørnøya, Svalbard: response to high frequency, high amplitude sea level fluctuations and local tectonism. *Polar Res.* 19, 227–249. <https://doi.org/10.3402/polar.v19i2.6548>.
- Suggate, R.P., 1998. Relations between Depth of Burial, Vitrinite Reflectance and Geothermal Gradient. *J. Petrol. Geol.* 21, 5–32. <https://doi.org/10.1111/j.1747-5457.1998.tb00644.x>.

- Sykes, R., Snowdon, L.R., 2002. Guidelines for assessing the petroleum potential of coaly source rocks using Rock-Eval pyrolysis. *Org. Geochem.* 33, 1441–1455. [https://doi.org/10.1016/s0146-6380\(02\)00183-3](https://doi.org/10.1016/s0146-6380(02)00183-3).
- Teichmüller, M., Durand, B., 1983. Fluorescence microscopical rank studies on liptinites and vitrinites in peat and coals, and comparison with results of the rock-eval pyrolysis. *Int. J. Coal Geol.* 2, 197–230. [https://doi.org/10.1016/0166-5162\(83\)90001-0](https://doi.org/10.1016/0166-5162(83)90001-0).
- Tsikalas, F., Blaich, O.A., Faleide, J.I., Olaussen, S., 2021. Stappen High-Bjørnøya Tectono-Sedimentary Element, Barents Sea. Geological Society, London, Memoirs 57. <https://doi.org/10.1144/m57-2016-24>.
- Tyson, R.V., 1995. *Sedimentary Organic Matter*. Chapman and Hill. <https://doi.org/10.1007/978-94-011-0739-6>.
- van Koeverden, J.H., Karlsen, D.A., Backer-Owe, K., 2011. Carboniferous Non-Marine Source Rocks from Spitsbergen and Bjørnøya: Comparison with the Western Arctic. *J. Petrol. Geol.* 34, 53–66. <https://doi.org/10.1111/j.1747-5457.2011.00493.x>.
- van Koeverden, J.H., Karlsen, D.A., Schwark, L., Chpitsglouz, A., Backer-Owe, K., 2010. Oil-Prone Lower Carboniferous Coals in the Norwegian Barents Sea: Implications for a Palaeozoic Petroleum System. *J. Petrol. Geol.* 33, 155–181. <https://doi.org/10.1111/j.1747-5457.2010.00471.x>.
- Vogt, T., 1941. Geology of a Middle Devonian cannel coal from Spitsbergen. *Norges geologisk tidsskrift* 21, 1–18.
- Volkova, I.B., 1994. Nature and Composition of the Devonian Coals of Russia. *Energy Fuel* 8, 1489–1493.
- Weiss, H.M., Wilhelms, A., Mills, N., Scotchmer, J., Hall, P.B., Lind, K., Brekke, T., 2000. NIGOGA - the Norwegian Industry Guide to Organic Geochemical Analyses, 4.0.
- Wesenlund, F., Grundvåg, S.-A., Engelschjøn, V.S., Thießen, O., Pedersen, J.H., 2021. Linking facies variations, organic carbon richness and bulk bitumen content – A case study of the organic-rich Middle Triassic shales from eastern Svalbard. *Mar. Petrol. Geol.* 132 <https://doi.org/10.1016/j.marpetgeo.2021.105168>.
- Wilkins, R.W.T., George, S.C., 2002. Coal as a source rock for oil: a review. *Int. J. Coal Geol.* 50, 317–361. [https://doi.org/10.1016/s0166-5162\(02\)00134-9](https://doi.org/10.1016/s0166-5162(02)00134-9).
- Worsley, D., Agdestein, T., Gjelberg, J.G., Kirkemo, K., Mørk, A., Nilsson, I., Olaussen, S., Steel, R.J., Stemmerik, L., 2001. The geological evolution of Bjørnøya, Arctic Norway: implications for the Barents Shelf. *Norw. J. Geol.* 81, 195–234.
- Worsley, D., Edwards, M.B., 1976. The Upper Palaeozoic succession of Bjørnøya. *Nor. Polarinst. Arbok* 1974, 17–34.